

UC Davis

UC Davis Previously Published Works

Title

Development of a radioligand for imaging V1a vasopressin receptors with PET

Permalink

<https://escholarship.org/uc/item/8bm3d0nn>

Authors

Naik, Ravi
Valentine, Heather
Hall, Andrew
[et al.](#)

Publication Date

2017-10-01

DOI

10.1016/j.ejmech.2017.08.037

Peer reviewed



Published in final edited form as:

Eur J Med Chem. 2017 October 20; 139: 644–656. doi:10.1016/j.ejmech.2017.08.037.

Development of a radioligand for imaging V_{1a} vasopressin receptors with PET

Ravi Naik[†], Heather Valentine[†], Andrew Hall[†], William B. Mathews[†], James C. Harris[†], C. Sue Carter[‡], Robert F. Dannals[†], Dean F. Wong[†], and Andrew G. Horti^{†,*}

[†]Department of Radiology, The Johns Hopkins University School of Medicine, Baltimore, 21287 USA

[‡]The Kinsey Institute, Indiana University, Bloomington, IN, 47405 USA

Abstract

A series of vasopressin receptor V_{1a} ligands have been synthesized for positron emission tomography (PET) imaging. The lead compound (1*S*,5*R*)-**1** ((4-(1Hindol-3-yl)-3-methoxyphenyl)((1*S*,5*R*)-1,3,3-trimethyl-6-azabicyclo[3.2.1]octan-6-yl)methanone) and its F-ethyl analog **6c** exhibited the best combination of high binding affinity and optimal lipophilicity within the series. (1*S*,5*R*)-**1** was radiolabeled with ¹¹C for PET studies. [¹¹CH₃](1*S*,5*R*)-**1** readily entered the mouse (4.7% ID/g tissue) and prairie vole brains (~2% ID/g tissue) and specifically (30–34%) labeled V_{1a} receptor. The common animal anesthetic Propofol significantly blocked the brain uptake of [¹¹CH₃](1*S*,5*R*)-**1** in the mouse brain, whereas anesthetics Ketamine and Saffan increased the uptake variability. Future PET imaging studies with V_{1a} radiotracers in non-human primates should be performed in awake animals or using anesthetics that do not affect the V_{1a} receptor.

Graphical Abstract

*Corresponding Author Phone: (1) 410-614-5130; ahorti1@jhmi.edu, Department of Radiology, The Johns Hopkins University School of Medicine, Baltimore, 21287 USA.

Author Contributions

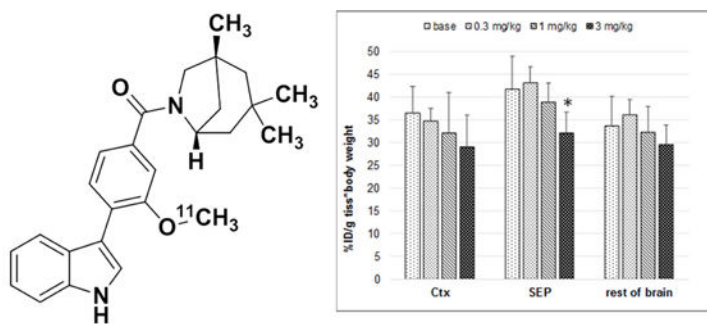
All authors have given approval to the final version of the manuscript.

*Present Address

Department of Radiology, The Johns Hopkins University School of Medicine, Baltimore, 21287 USA.

Publisher's Disclaimer: This is a PDF file of an unedited manuscript that has been accepted for publication. As a service to our customers we are providing this early version of the manuscript. The manuscript will undergo copyediting, typesetting, and review of the resulting proof before it is published in its final form. Please note that during the production process errors may be discovered which could affect the content, and all legal disclaimers that apply to the journal pertain.

The authors declare no competing financial interest.



$[^{11}\text{C}]_3(1S,5R)\text{-1}$ specifically labels V_{1a} receptors *in vivo* in the rodent brain

Keywords

Vasopressin receptor; positron emission tomography; radiotracers

1. INTRODUCTION:

Arginine vasopressin (AVP) is essential for a wide range of physiological functions in the periphery and central nervous system (CNS). In the periphery, AVP works as a hormone that regulates water reabsorption, blood pressure, cardiovascular homeostasis, hormone secretion [1, 2]. In the CNS, AVP acts as a neuromodulator that activates various brain regions through binding to vasopressin receptors involved in the regulation of social, emotional and cognitive behaviors [3]. Social attunement is fundamental to sexual behavior, pair-bonding, maternal behavior, mate guarding, social memory and biparental care [4, 5]. The role of AVP in human social behavior [6–9] is an emerging area of research in autism spectrum disorder (ASD) [10, 11].

The action of AVP is mediated by three known G-protein-coupled receptor subtypes: V_{1a} , V_{1b} , and V_2 (see for review) [6]. The receptors V_{1a} and V_{1b} are expressed in the CNS, but there is no clear evidence of the expression of V_2 in the brain of mammals [6, 12–15]. Many social behavioral effects of AVP are primarily mediated by V_{1a} receptor [6–9, 16–19]. This is pertinent to ASD where blockade of the V_{1a} receptor may improve social communication in adults with high-functioning ASD [20].

In vivo imaging and quantification of V_{1a} receptors in human brain could provide an important advance in the understanding of ASD and other neuropsychiatric disorders related to this vasopressin receptor subtype and potentially facilitate the development of novel V_{1a} drugs.

Such studies may be conducted using positron emission tomography (PET). PET is an advanced technique to quantify neuronal receptors and their occupancy *in vivo*. The development of a PET radiotracer for V_{1a} imaging is of considerable importance, however, the development of a PET radioligand suitable for quantification of the V_{1a} receptor in healthy and diseased brains remains challenging.

A previous study [21] described the first V_{1a} PET radiotracers, but imaging studies in animals with these radiotracers have not been reported, possibly because of the suboptimal molecular weights (700–800 Dalton) of the radiotracers for sufficient blood-brain barrier permeability.

We aimed to develop a small molecule PET radiotracer based on the scaffold of compound (1*S*,5*R*)-**1** (Fig. 1), a high affinity and selective V_{1a} antagonist ($K_i^{V_{1a}} = 0.1$ nM; $K_i^{V_2} = 600$ nM) developed by Pfizer [22]. In this report, we describe the design, synthesis, radiolabeling and *in vitro* and *in vivo* characterization in mice of a series of high V_{1a} binding affinity derivatives of **1** as potential probes for PET imaging of V_{1a} receptors.

2. RESULTS AND DISCUSSION

2.1. Chemistry:

A series of V_{1a} ligands was synthesized as shown in Schemes 1–4. The synthesis of key intermediates, racemic 4-iodo-phenyl-(1,3,3-trimethyl-6-aza-bicyclo[3.2.1]octan-6-yl)methanone derivatives **3** including the previously published **3a**, [22] is summarized in Scheme 1.

The first group of V_{1a} ligands **1**, **6a–b** was synthesized in a high yield by the Suzuki reaction [20] of racemic iodo-arenes **3a–c** and *tert*-butyl 3-(4,4,5,5-tetramethyl-1,3,2-dioxaborolan-2-yl)-1*H*-indole-1-carboxylate **4** followed by cleavage of the *tert*-Boc-group. The hydroxyl compound **6a** reacted with 2fluoroethyl tosylate in the presence of Cs_2CO_3 in DMF to give the fluoroethyl compound **6c** in high yield (Scheme 2).

Racemic **1** was separated into two enantiomers (1*S*,5*R*)-**1** and (1*R*,5*S*)-**1** [22] by preparative chiral HPLC. Compound **6a** was also separated in two enantiomers (1*S*,5*R*)-**6a** and (1*R*,5*S*)-**6a** using chiral supercritical fluid chromatography.

Synthesis of compounds **8a–l** was achieved by the Suzuki reaction of the iodo-intermediates **3a**, **3c–d** with commercially available boronic acids or in-house prepared boronic esters **7** (Scheme 3) [21].

Compounds **13a–e** were prepared in four steps as shown in Scheme 4. The Suzuki cross-coupling reaction between methyl 4-bromo-3-methoxybenzoate **9** and *tert*-butyl 3-(4,4,5,5-tetramethyl-1,3,2-dioxaborolan-2-yl)-1*H*-indole-1-carboxylate **4** led to the formation of the benzoic ester derivative **10** in an excellent yield. The ester derivative **10** underwent *tert*-Boc deprotection followed by saponification with aqueous LiOH to yield the carboxylic acid derivative **12**. Coupling of **12** with various amines led to the desired amide derivatives **13a–e**.

2.2. Structure–Activity Relationship:

The purpose of the study was to develop a V_{1a} ligand with high V_{1a} receptor binding affinity and suitable molecular properties for brain PET (molecular weight MW < 500 Dalton, lipophilicity $\log D < 5$). In addition, the suitable ligand structures have to possess a fluorine atom or methyl group for ^{18}F - or ^{11}C -radiolabeling.

The high binding affinity requirement is a crucial component in the PET radiotracer development and is based on the conventional equation $\frac{B_{max}}{K_D} > 10$, where B_{max} is receptor density in the brain tissue and K_D is the dissociation constant [23]. In many reports, the V_{1a} receptor density in the brain tissue of various species was determined semi-quantitatively [15, 24]. The quantitatively determined V_{1a} density value (B_{max}) in the mammalian brain varies substantially among different reports, perhaps due to the high nonspecific binding and insufficient selectivity of the available *in vitro* radiotracers that were used in the assays: in rat – 4 fmol/mg protein [25], 10–15 fmol/mg protein [26], 20–80 fmol/mg protein [13], 150–408 fmol/mg protein [27]; in golden hamster – 12 fmol/mg protein [28]. The required binding affinity for a good V_{1a} PET radiotracer should be in the range of $K_i < 0.4 - 40$ nM, but the deficiency of the *in vitro* binding assay makes this estimate rather imprecise. Based on the above approximation of the required binding affinity and other structural properties, the V_{1a} ligand (1*S*,5*R*)-**1** ($K_i = 0.1$ nM, MW = 402, logD = 4.7) was selected as a lead for this project. The binding affinity of the lead was confirmed in this study (see Table 1).

The overall objective of this research was to synthesize a series of analogs of **1** with appropriate characteristics for brain PET radiotracer including high binding affinity $K_i < 0.4 - 40$ nM) (see previous paragraph for the rational). The other necessary properties for cerebral PET tracer include optimal lipophilicity (logD < 5) and molecular weight MW < 500 Dalton [29, 30].

The fluoro derivatives **6b**, **8a**, and **8b** exhibited satisfactory lipophilicity, but lower binding affinity compared to the lead **1** (Table 1).

The fluoroethyl-analog **6c** manifested high binding affinity and lipophilicity that was comparable to the lead **1**. The derivative **8c**, synthesized by *N*-methylation of **1**, resulted to an increase of lipophilicity and decrease in binding affinity.

Azaindole derivatives **8d-8f** exhibited an optimal lipophilicity, but the binding affinities were lower than that of **1**.

Interestingly, tolyl derivatives **8g** and **8k**, those are less bulky than **1**, exhibited good binding affinity, whereas the picolyl derivatives (**8h-j** and **8l**) showed poor V_{1a} binding affinity (Table 1).

Replacement of the 1,3,3-trimethyl-6-aza-bicyclo[3.2.1]octan-6-yl moiety in compounds **13a-e** with other cyclic amines substituents resulted in a loss of the V_{1a} binding affinity (Table 2).

2.3. Radiochemistry:

Two compounds of the series, the lead (1*S*,5*R*)-**1** and its F-ethyl analog **6c**, exhibited the best combination of high binding affinity and optimal lipophilicity (Table 1) and were suitable for PET radiolabeling with ^{11}C and ^{18}F , respectively. Because of relative simplicity of ^{11}C radiolabeling we have chosen to radiolabel (1*S*,5*R*)-**1** with ^{11}C for further animal experiments. Radiolabelled [^{11}C CH₃](1*S*,5*R*)-**1** was prepared by ^{11}C -methylation of the corresponding phenol precursor (1*S*,5*R*)-**6a** (Scheme 5). The precursor (1*S*,5*R*)-**6a** (ee

–99.5%) was obtained by supercritical fluid chiral chromatographic separation of racemic **6a**. [$^{11}\text{CH}_3$](1*S*,5*R*)-**1** was prepared with a radiochemical yield of 10–15%, specific radioactivity 8000 – 16000 mCi/ μmol (296 – 590 GBq/ μmol) and radiochemical purity > 95%. The enantiomeric purity (e.e.>95%) of [$^{11}\text{CH}_3$](1*S*,5*R*)-**1** was demonstrated by chiral HPLC analysis.

Radiotracer [$^{11}\text{CH}_3$](1*S*,5*R*)-**1** undergoes a rapid radiolysis in saline solution, but it is stable for at least 1 h in saline solution containing 7–8% alcohol.

2.4. Biodistribution studies in rodents.

Radioligand [$^{11}\text{CH}_3$](1*S*,5*R*)-**1** was evaluated in rodents as a potential PET radiotracer for imaging V_{1a} receptors.

2.4.1. Baseline studies in CD-1 mice.—After intravenous injection [$^{11}\text{CH}_3$](1*S*,5*R*)-**1** manifested high initial brain uptake with peak concentration of radioactivity at 5 min post-injection (4.7 %ID/g tissue) followed by washout. The lateral septum was the region with the highest accumulation of radioactivity, which is consistent with previous *in vitro* semi-quantitative autoradiography results in C57B6 mice [31]. The uptake in the hippocampus, cortex, and the rest of brain was lower than that in the septum (Table 3).

2.4.2. Dose-Escalation Blocking in CD-1 Mice.—In all studied brain regions (septum, hippocampus, cortex) at 60 min after injection of [$^{11}\text{CH}_3$](1*S*,5*R*)-**1**, radiotracer binding was blocked by injection of V_{1a} ligand **8g** ($K_i = 0.05$ nM) [22] in a dose-dependent fashion (Fig. 2). At the highest blocker dose of 3 mg/kg, the reduction of radioactivity uptake in the septum, cortex, and rest of brain was 30%, 26%, and 14%, respectively. The blockade in the septum was significant, suggesting that [$^{11}\text{CH}_3$](1*S*,5*R*)-**1** specifically labels V_{1a} receptors in this brain region.

2.4.3. Brain regional biodistribution studies in male prairie voles.—Previous studies revealed an involvement of V_{1a} receptor in mediation of paternal behavior, selective aggression and affiliation in monogamous rodent species including prairie voles [12], Taiwan voles [32] and deer mice [33]. We examined the regional distribution of [$^{11}\text{CH}_3$](1*S*,5*R*)-**1** in male prairie voles. The uptake of [$^{11}\text{CH}_3$](1*S*,5*R*)-**1** was higher in the superior colliculus and thalamus and lower in the cortex and rest of brain (Fig. 3). This distribution of the radiotracer is in agreement with the *in vitro* distribution of V_{1a} in the prairie voles [12]. The uptake of the radiotracer [$^{11}\text{CH}_3$](1*S*,5*R*)-**1** was reduced in the blocking studies with **1**. The blocking was significant only in the superior colliculus (Fig. 3), the region with the greatest density of V_{1a} [12].

2.4.4. Effect of anesthetics.—Previous research established that common animal anesthetics such as Propofol [34] and NMDA antagonists [35] interact with the vasopressin receptor system and alter the binding of V_{1a} receptors. Because in our lab we commonly use Propofol and an NMDA antagonist Ketamine as anesthetics for baboon PET imaging, we investigated an effect of these anesthetics and another common animal anesthetic Saffron on the brain regional biodistribution of [$^{11}\text{CH}_3$](1*S*,5*R*)-**1** in mice.

The study demonstrated that intraperitoneal treatment of CD-1 mice with all three anesthetics greatly increased the variability of the radiotracer brain uptake as compared with controls (28–43% (anesthetics); 0.4–3.5% (controls)) (Fig. 4). The study showed a significant reduction of the radiotracer uptake in the hippocampus in the mice treated with Propofol and insignificant reduction in other brain regions. Ketamine and Saffan treatment did not significantly change the radiotracer brain uptake. However, in the case of Saffan, there was a trend toward a decrease in the uptake. Saffan is composed of two neuroactive steroids alfaxalone and alfadolone (3:1). Neuroactive steroids are known to modulate the secretion of vasopressin [36] and, thus, may affect the V_{1a} receptor radiotracer binding.

The results of this study and previous research [34] suggest that Propofol blocks the V_{1a} and may be unsuitable as an anesthetic for future vasopressin receptor PET imaging in non-human primates. The high variability of the radiotracer uptake in the Saffan and ketamine experiments demonstrated that these two anesthetics are not benign for V_{1a} receptor imaging and different classes of anesthetics should be considered.

3. CONCLUSIONS

A novel series of V_{1a} receptor ligands has been developed for PET imaging. The lead ligand (1*S*,5*R*)-**1** with the best binding affinity (0.66 nM) was radiolabeled with ^{11}C for positron emission tomography studies. [$^{11}\text{CH}_3$](1*S*,5*R*)-**1** readily entered the mouse (4.7% ID/g tissue) and prairie vole brains (~2% ID/g tissue) and specifically (30 – 34%) labeled V_{1a} receptors. The common animal anesthetic Propofol significantly blocks the brain uptake of [$^{11}\text{CH}_3$](1*S*,5*R*)-**1** in the mouse brain, whereas anesthetics Ketamine and Saffan increase the variability of uptake. Future PET imaging studies with [$^{11}\text{CH}_3$](1*S*,5*R*)-**1** or other V_{1a} radiotracers in non-human primates should be performed in awake animals or use anesthetics that do not affect the V_{1a} receptor. Such studies are needed to advance our understanding of the role of V_{1a} receptor in social behavior.

4. EXPERIMENTAL SECTION:

All reagents were used directly as obtained commercially unless otherwise noted. Reaction progress was monitored by thin-layer chromatography (TLC) using silica gel 60 F254 (0.040–0.063 mm) with detection by UV. All moisture-sensitive reactions were performed under an argon atmosphere using oven-dried glassware and anhydrous solvents. Column flash chromatography was carried out using BDH silica gel 60Å (40–63 micron). Analytical TLC was performed on plastic sheets coated with silica gel 60 F254 (0.25 mm thickness, E. Merck, Darmstadt, Germany). ^1H NMR spectra were recorded with a Bruker-500 NMR spectrometer at nominal resonance frequencies of 500 MHz in CDCl_3 , CD_3OD or $\text{DMSO}-d_6$ (referenced to internal Me_4Si at δ 0 ppm). The chemical shifts (δ) were expressed in parts per million (ppm). High-resolution mass spectra were recorded utilizing electrospray ionization (ESI) at the University of Notre Dame Mass Spectrometry facility. All compounds that were tested in the biological assays were analyzed by combustion analysis (CHN) to confirm a purity of >95%. A dose calibrator (Capintec 15R) was used for all radioactivity measurements. Radiolabelling was performed with a modified GE MicroLab radiochemistry

box. The experimental animal protocols were approved by the Animal Care and Use Committee of the Johns Hopkins Medical Institutions.

4.1. Chemistry

(4-Iodo-3-methoxyphenyl)(1,3,3-trimethyl-6-aza-bicyclo[3.2.1]octan-6-yl)methanone (3a): To the mixture of 4-iodo-3-methoxybenzoic acid (**1a**) (1.0 g, 3.60 mmol), 1,3,3-trimethyl-6-azabicyclo[3.2.1]octane (0.55 g, 3.60 mmol), EDC.HCl (0.83 g, 4.32 mmol), and HOBT (0.58 g, 4.32 mmol), in DMF (10 mL) was added *N,N*-Diisopropylethylamine (DIEA) (1.25 mL, 7.20 mmol). The reaction mixture was stirred at room temperature overnight and then partitioned between EtOAc and brine. The organic layer was separated, dried over anhydrous MgSO₄, filtered, and concentrated under a vacuum. The resulting residue was purified by silica gel column chromatography (Hexane:EtOAc = 3:7) to give (4-iodo-3-methoxyphenyl)(1,3,3-trimethyl-6-aza-bicyclo[3.2.1]octan-6-yl)methanone as a white solid (1.12 g, 75.4% yield). ¹H NMR (500 MHz, CDCl₃) δ 7.57 (t, *J* = 5.0 Hz, 1H), 7.02 (d, *J* = 10.0 Hz, 1H), 6.93 (d, *J* = 10.0 Hz, 1H), 4.00 (t, *J* = 5.0 Hz, 1H), 3.93 (s, 3H), 3.60 (t, *J* = 5.0 Hz, 1H), 3.30 (t, *J* = 5.0 Hz, 1H), 2.27–2.24 (m, 1H), 1.81–1.77 (m, 1H), 1.62–1.60 (m, 1H), 1.50–1.47 (m, 1H), 1.38–1.34 (m, 2H), 1.25 (d, *J* = 10.0 Hz, 1H), 1.16 (s, 3H), 1.06 (s, 3H), 0.98 (d, *J* = 10.0 Hz, 3H).

(3-Hydroxy-4-iodophenyl)(1,3,3-trimethyl-6-aza-bicyclo[3.2.1]octan-6-yl)methanone (3b): To the mixture of 3-hydroxy-4-iodobenzoic acid (**1b**) (1.0 g, 3.78 mmol), 1,3,3-trimethyl-6-azabicyclo[3.2.1]octane (0.58 g, 3.78 mmol), EDC.HCl (0.87 g, 4.53 mmol), and HOBT (0.61 g, 4.53 mmol), in DMF (10 mL) was added DIEA (1.31 mL, 7.56 mmol). The reaction mixture was stirred at room temperature overnight and then partitioned between EtOAc and brine. The organic layer was separated, dried over anhydrous MgSO₄, filtered, and concentrated under a vacuum. The resulting residue was purified by silica gel column chromatography (Hexane:EtOAc = 3:7) to give (3hydroxy-4iodophenyl)(1,3,3-trimethyl-6-aza-bicyclo[3.2.1]octan-6-yl)methanone as a white solid (1.20 g, 80.6% yield). ¹H NMR (500 MHz, CDCl₃) δ 7.78 (s, 1H), 7.66 (d, *J* = 10.0 Hz, 1H), 7.08–7.04 (m, 1H), 6.69–6.65 (m, 1H), 4.59 (t, *J* = 5.0 Hz, 1H), 3.60 (t, *J* = 5.0 Hz, 1H), 3.26–3.23 (m, 1H), 1.76–1.74 (m, 1H), 1.57 (d, *J* = 10.0 Hz, 1H), 1.48–1.41 (m, 2H), 1.38–1.30 (m, 2H), 1.19 (d, *J* = 10.0 Hz, 1H), 1.08 (s, 3H), 1.00 (s, 3H), 0.93 (d, *J* = 10.0 Hz, 3H).

(2-Fluoro-4-iodophenyl)(1,3,3-trimethyl-6-aza-bicyclo[3.2.1]octan-6-yl)methanone (3c): To the mixture of 2-fluoro-4-iodobenzoic acid (**1c**) (1.0 g, 3.75 mmol), 1,3,3-trimethyl-6-azabicyclo[3.2.1]octane (0.58 g, 3.75 mmol), EDC.HCl (0.86 g, 4.50 mmol), and HOBT (0.61 g, 4.50 mmol), in DMF (10 mL) was added DIEA (1.31 mL, 7.50 mmol). The reaction mixture was stirred at room temperature overnight and then partitioned between EtOAc and brine. The organic layer was separated, dried over anhydrous MgSO₄, filtered, and concentrated under a vacuum. The resulting residue was purified by silica gel column chromatography (Hexane:EtOAc = 4:6) to give (2fluoro-4iodophenyl)(1,3,3-trimethyl-6-aza-bicyclo[3.2.1]octan-6-yl)methanone as a white solid (1.25 g, 82.9% yield). ¹H NMR (500 MHz, CDCl₃) δ 7.36–7.33 (m, 1H), 7.32–7.28 (m, 1H), 7.24–7.20 (m, 1H), 4.65 (t, *J* = 5.0 Hz, 1H), 3.64 (t, *J* = 5.0 Hz, 1H), 3.26 (t, *J* = 5.0

Hz, 1H), 3.23–3.08 (m, 1H), 1.82–1.79 (m, 1H), 1.48–1.47 (m, 1H), 1.44–1.41 (m, 2H), 1.38–1.32 (m, 2H), 1.17 (d, $J = 10.0$ Hz, 1H), 1.10 (s, 3H), 1.04 (s, 3H), 0.94 (d, $J = 10.0$ Hz, 3H).

(4-Iodophenyl)(1,3,3-trimethyl-6-aza-bicyclo[3.2.1]octan-6-yl)methanone

(3d): To the mixture of 4iodobenzoic acid (**1d**) (1.0 g, 4.03 mmol), 1,3,3-trimethyl-6-azabicyclo[3.2.1]octane (0.62 g, 4.03 mmol), EDC.HCl (0.92 g, 4.83 mmol), and HOBT (0.65 g, 4.83 mmol), in DMF (10 mL) was added DIEA (1.50 mL, 8.60 mmol). The reaction mixture was stirred at room temperature overnight and then partitioned between EtOAc and brine. The organic layer was separated, dried over anhydrous $MgSO_4$, filtered, and concentrated under a vacuum. The resulting residue was purified by silica gel column chromatography (Hexane:EtOAc = 4:6) to give (4-iodophenyl)(1,3,3-trimethyl-6-azabicyclo[3.2.1]octan-6-yl)methanone as a white solid (1.30 g, 84.4% yield). 1H NMR (500 MHz, $CDCl_3$) δ 7.56 (t, $J = 10.0$ Hz, 2H), 7.35 (d, $J = 10.0$ Hz, 2H), 3.96 (t, $J = 5.0$ Hz, 1H), 3.61 (d, $J = 10.0$ Hz, 1H), 3.30 (t, $J = 5.0$ Hz, 1H), 2.27–2.24 (m, 1H), 1.80–1.77 (m, 1H), 1.62–1.54 (m, 2H), 1.49–1.44 (m, 1H), 1.40–1.33 (m, 1H), 1.23 (d, $J = 10.0$ Hz, 1H), 1.15 (s, 3H), 1.05 (s, 3H), 0.97 (d, $J = 10.0$ Hz, 3H).

***Tert*-butyl 3-(2methoxy-4-(1,3,3-trimethyl-6-aza-bicyclo[3.2.1]octane-6-carbonyl)phenyl)-1Hindole-1-carboxylate (5a):**

To a solution of (4-iodo-3-methoxyphenyl)(1,3,3-trimethyl-6-azabicyclo[3.2.1]octan-6-yl)methanone (**3a**) (0.3 g, 0.72 mmol) and *tert*-butyl 3-(4,4,5,5-tetramethyl-1,3,2dioxaborolan-2-yl)-1H-indole-1-carboxylate (**4**) (0.27 g, 0.80 mmol) in 1,4-dioxane (4.0 mL) was added 1.0 mL of water. The reaction mixture was degassed with argon for about 30 minutes. After that $Pd(dppf)Cl_2.DCM$ (0.03 g, 0.036 mmol) and Na_2CO_3 (0.15 g, 1.45 mmol) were added to the reaction mixture and again degassed with argon for another 20 minutes. The reaction mixture was stirred under reflux for 3 h. After cooled down to room temperature, the mixture was extracted with EtOAc, washed with brine, dried over Na_2SO_4 , and concentrated under reduced pressure. The crude product was purified by column chromatography (Hexane/EtOAc = 3:7) to afford **5a** as a brown solid (0.32 g, 87.9%). 1H NMR (500 MHz, $CDCl_3$) δ 8.22 (d, $J = 10.0$ Hz, 1H), 7.82 (s, 1H), 7.60 (d, $J = 5.0$ Hz, 1H), 7.56 (d, $J = 5.0$ Hz, 1H), 7.55–7.53 (m, 1H), 7.36 (s, 1H), 7.27 (d, $J = 5.0$ Hz, 1H), 7.13 (d, $J = 10.0$ Hz, 1H), 4.68 (s, 1H), 3.89 (s, 3H), 3.64 (d, $J = 10.0$ Hz, 1H), 3.43–3.40 (m, 1H), 3.28 (d, $J = 5.0$ Hz, 1H), 2.32–2.29 (m, 1H), 1.84–1.82 (m, 1H), 1.76–1.73 (m, 2H), 1.71 (s, 9H), 1.60 (s, 1H), 1.54–1.47 (m, 1H), 1.43–1.37 (m, 1H), 1.20 (s, 3H), 1.10 (s, 3H), 1.00 (d, $J = 10.0$ Hz, 3H).

***Tert*-butyl 3-(2hydroxy-4-(1,3,3-trimethyl-6-aza-bicyclo[3.2.1]octane-6-carbonyl)phenyl)-1Hindole-1-carboxylate (5b):**

To a solution of (3hydroxy-4-iodophenyl)(1,3,3-trimethyl-6-azabicyclo[3.2.1]octan-6-yl)methanone (**3b**) (0.5 g, 1.25 mmol) and *tert*-butyl 3-(4,4,5,5-tetramethyl-1,3,2dioxaborolan-2-yl)-1H-indole-1-carboxylate (**4**) (0.47 g, 1.38 mmol) in 1,4-dioxane (10.0 mL) was added 2.0 mL of water. The reaction mixture was degassed with argon for about 30 minutes. After that $Pd(dppf)Cl_2.DCM$ (0.05 g, 0.063 mmol) and Na_2CO_3 (0.26 g, 2.50 mmol) were added to the reaction mixture and again degassed with argon for another 20 minutes. The reaction mixture was stirred under reflux for 3 h. After cooled down to room temperature, the mixture was extracted with

EtOAc, washed with brine, dried over Na₂SO₄, and concentrated under reduced pressure. The crude product was purified by column chromatography (Hexane/EtOAc =3:7) to afford **5b** as a brown solid (0.48 g, 78.5%). ¹H NMR (500 MHz, CDCl₃) δ 8.26 (d, *J*= 10.0 Hz, 1H), 7.81(s, 1H), 7.59–7.56 (m, 1H), 7.46–7.40 (m, 2H), 7.30 (d, *J*= 10.0 Hz, 1H), 7.22 (d, *J*= 10.0 Hz, 1H), 7.11–7.06 (m, 1H), 4.68 (s, 1H), 3.64 (d, *J*= 10.0 Hz,

1H), 3.43–3.40 (m, 1H), 3.28 (d, *J*= 5.0 Hz, 1H), 2.32–2.29 (m, 1H), 1.84–1.82 (m, 1H), 1.76–1.73 (m, 2H), 1.72 (s, 9H), 1.60 (s, 1H), 1.54–1.47 (m, 1H), 1.43–1.37 (m, 1H), 1.28 (s, 3H), 1.15 (s, 3H), 1.09 (d, *J*= 10.0 Hz, 3H).

Tert-butyl 3-(3fluoro-4-(1,3,3-trimethyl-6-aza-bicyclo[3.2.1]octane-6-carbonyl)phenyl)-1H-indole-1-carboxylate (5c): To a solution of (2-fluoro-4-iodophenyl)(1,3,3-trimethyl-6-aza-bicyclo[3.2.1]octan-6-yl)methanone (**3c**) (0.3 g, 0.75 mmol) and *tert*-butyl 3-(4,4,5,5-tetramethyl-1,3,2-dioxaborolan-2-yl)1H-indole-1-carboxylate (**4**) (0.28 g, 0.82 mmol) in 1,4-dioxane (4.0 mL) was added 1.0 mL of water. The reaction mixture was degassed with argon for about 30 minutes. After that Pd(dppf)Cl₂.DCM (0.030 g, 0.037 mmol) and Na₂CO₃ (0.16 g, 1.50 mmol) were added to the reaction mixture and again degassed with argon for another 20 minutes. The reaction mixture was stirred under reflux for 3 h. After cooled down to room temperature, the mixture was extracted with EtOAc, washed with brine, dried over Na₂SO₄, and concentrated under reduced pressure. The crude product was purified by column chromatography (Hexane/EtOAc = 3:7) to afford **5c** as a brown solid (0.31 g, 84.7%). ¹H NMR (500 MHz, CDCl₃) δ 8.26 (d, *J*= 10.0 Hz, 1H), 7.81(s, 1H), 7.59–7.56 (m, 1H), 7.46–7.40 (m, 2H), 7.30 (d, *J*= 10.0 Hz, 1H), 7.22 (d, *J*= 10.0 Hz, 1H), 7.11–7.06 (m, 1H), 4.68 (s, 1H), 3.64 (d, *J*= 10.0 Hz, 1H), 1.43–1.40 (m, 1H), 3.28 (d, *J*= 5.0 Hz, 1H), 2.32–2.29 (m, 1H), 1.84–1.82 (m, 1H), 1.76–1.73 (m, 2H), 1.72 (s, 9H), 1.60 (s, 1H), 1.54–1.47 (m, 1H), 1.43–1.37 (m, 1H), 1.28 (s, 3H), 1.15 (s, 3H), 1.09 (d, *J*= 10.0 Hz, 3H).

(4-(1H-Indol-3-yl)-3-methoxyphenyl)(1,3,3-trimethyl-6-aza-bicyclo[3.2.1]octan-6-yl)methanone (1): To a solution of *tert*-butyl 3-(2-methoxy-4-(1,3,3-trimethyl-6-aza-bicyclo[3.2.1]octane-6-carbonyl)phenyl)-1H-indole-1-carboxylate (**5a**) (0.47 g, 0.935 mmol) in methylene chloride (5 mL) was added trifluoroacetic acid (0.29 mL, 3.74 mmol) dropwise at 0 °C, and then, the mixture was stirred at room temperature for 8 h. After completion of the reaction, the reaction mixture was concentrated under reduced pressure. The resulting residue was purified by silica gel column chromatography (Hexane:EtOAc = 2:8) to give (4-(1H-indol-3-yl)-3-methoxyphenyl)(1,3,3-trimethyl-6-azabicyclo[3.2.1]octan-6-yl)methanone as a pale yellow solid (0.32 g, 85.1% yield). ¹H NMR (500 MHz, CDCl₃) δ 8.38 (d, *J*= 10.0 Hz, 1H), 7.81 (d, *J*= 10.0 Hz, 1H), 7.68 (d, *J*= 10.0 Hz, 1H), 7.57 (s, 1H), 7.45 (d, *J*= 5.0 Hz, 1H), 7.27 (d, *J*= 5.0 Hz, 1H), 7.19–7.14 (m, 3H), 4.68 (s, 1H), 3.90 (s, 3H), 3.64 (d, *J*= 10.0 Hz, 1H), 3.39–3.30 (m, 1H), 1.85–1.82 (m, 1H), 1.79–1.76 (m, 1H), 1.66 (d, *J*= 10.0 Hz, 1H), 1.54–1.47 (m, 2H), 1.41–1.36 (m, 1H), 1.30–1.27 (m, 1H), 1.20 (s, 3H), 1.12 (s, 3H), 1.00 (d, *J*= 10.0 Hz, 3H). ¹³CNMR (125 MHz, CDCl₃) δ 170.0, 156.4, 136.1, 129.9, 126.4, 124.9, 122.1, 120.3, 120.1, 118.9, 118.6, 112.4, 111.4, 110.1, 109.7, 58.3, 56.7, 55.6, 44.5, 44.1, 38.5, 36.3, 31.2, 30.3, 25.2. HRMS (ESI+) *m/z* calcd [C₂₆H₃₁N₂O₂] [(M + H)]⁺ 403.2386, found 403.2380.

(3-Hydroxy-4-(1H-Indol-3-yl)phenyl)(1,3,3-trimethyl-6-aza-bicyclo[3.2.1]octan-6-yl)methanone (6a): To a solution of *tert*-butyl 3-(2-hydroxy-4-(1,3,3-trimethyl-6-aza-bicyclo[3.2.1]octane-6-carbonyl)phenyl)-1H-indole-1-carboxylate (**5b**) (0.3 g, 0.61 mmol) in methylene chloride (3 mL) was added trifluoroacetic acid (0.19 mL, 2.45 mmol) dropwise at 0 °C, and then, the mixture was stirred at room temperature for 8 h. After completion of the reaction, the reaction mixture was concentrated under reduced pressure. The resulting residue was purified by silica gel column chromatography (Hexane:EtOAc = 2:8) to give (4-(1H-indol-3-yl)-3-methoxyphenyl)(1,3,3-trimethyl-6-azabicyclo[3.2.1]octan-6-yl)methanone as a white solid (0.2 g, 84.0% yield). ¹H NMR (500 MHz, CDCl₃) δ 8.72 (d, *J* = 10.0 Hz, 1H), 7.68 (d, *J* = 10.0 Hz, 1H), 7.50 (d, *J* = 10.0 Hz, 2H), 7.30 (d, *J* = 5.0 Hz, 1H), 7.28 (d, *J* = 5.0 Hz, 1H), 7.19 (d, *J* = 10.0 Hz, 2H), 7.10–7.06 (m, 1H), 4.68 (s, 1H), 3.90 (s, 3H), 3.64 (d, *J* = 10.0 Hz, 1H), 3.30 (d, *J* = 10.0 Hz, 1H), 1.84–1.74 (m, 2H), 1.62 (d, *J* = 10.0 Hz, 1H), 1.55–1.45 (m, 2H), 1.39–1.35 (m, 1H), 1.29–1.26 (m, 1H), 1.17 (s, 3H), 1.09 (s, 3H), 0.98 (d, *J* = 10.0 Hz, 3H). ¹³C NMR (125 MHz, CDCl₃) δ 169.5, 153.4, 137.0, 136.5, 130.6, 126.1, 123.9, 122.8, 120.5, 119.7, 118.4, 114.0, 113.7, 111.7, 111.3, 64.5, 58.1, 56.4, 49.6, 38.5, 32.2, 30.0, 27.7, 25.4. HRMS (ESI+) *m/z* calcd [C₂₅H₂₉N₂O] [(M + H)⁺] 389.2229, found 389.2223.

(2-Fluoro-4-(1H-Indol-3-yl)phenyl)(1,3,3-trimethyl-6-aza-bicyclo[3.2.1]octan-6-yl)methanone (6b): To a solution of *tert*-butyl 3-(3-fluoro-4-(1,3,3-trimethyl-6-aza-bicyclo[3.2.1]octane-6-carbonyl)phenyl)-1H-indole-1-carboxylate (**5c**) (0.3 g, 0.61 mmol) in methylene chloride (25 mL) was added trifluoroacetic acid (0.19 mL, 2.44 mmol) dropwise at 0 °C, and then, the mixture was stirred at room temperature for 8 h. After completion of the reaction, the reaction mixture was concentrated under reduced pressure. The resulting residue was purified by silica gel column chromatography (Hexane:EtOAc = 2:8) to give (4-(1H-indol-3-yl)-3-methoxyphenyl)(1,3,3-trimethyl-6-azabicyclo[3.2.1]octan-6-yl)methanone as a brown solid (0.19 g, 79.8% yield). ¹H NMR (500 MHz, CDCl₃) δ 8.48 (s, 1H), 7.93 (d, *J* = 5.0 Hz, 1H), 7.49–7.44 (m, 2H), 7.39–7.37 (m, 3H), 7.28 (d, *J* = 5.0 Hz, 1H), 7.24–7.21 (m, 1H), 4.65 (s, 1H), 3.68 (d, *J* = 10.0 Hz, 1H), 3.30 (d, *J* = 10.0 Hz, 1H), 1.87–1.83 (m, 1H), 1.62 (d, *J* = 10.0 Hz, 1H), 1.55–1.45 (m, 2H), 1.39–1.34 (m, 2H), 1.22 (s, 1H), 1.14 (s, 3H), 1.09 (s, 3H), 0.95 (d, *J* = 10.0 Hz, 3H). HRMS (ESI+) *m/z* calcd [C₂₅H₂₈FN₂O] [(M + H)⁺] 391.2186, found 391.2180.

(3-(2-fluoroethoxy)-4-(1H-indol-3-yl)phenyl)(1,3,3-trimethyl-6-aza-bicyclo[3.2.1]octan-6-yl)methanone (6c): To a solution of (3-Hydroxy-4-(1H-Indol-3-yl)phenyl)(1,3,3-trimethyl-6-azabicyclo[3.2.1]octan-6-yl)methanone (**6a**) (0.1 g, 0.25 mmol) in DMF (1 mL) was added 2-Fluoroethyl tosylate (0.06 g, 0.28 mmol) and Cs₂CO₃ (0.125 g, 0.38 mmol). The reaction mixture was stirred at room temperature overnight and then partitioned between EtOAc and brine. The organic layer was separated, dried over anhydrous MgSO₄, filtered, and concentrated under a vacuum. The resulting residue was purified by silica gel column chromatography (EtOAc : Hexane = 7:3) to give **6c** as a white solid (0.06 g, 54.05% yield). ¹H NMR (500 MHz, CDCl₃) δ 8.51 (s, 1H), 7.88 (d, *J* = 5.0 Hz, 1H), 7.78–7.76 (m, 2H), 7.68 (s, 1H), 7.46 (d, *J* = 10.0 Hz, 1H), 7.27–7.13 (m, 4H), 4.76 (t, *J* = 5.0 Hz, 2H), 4.65 (s, 1H), 4.29 (t, *J* = 5.0 Hz, 2H), 3.68 (d, *J* = 10.0 Hz, 1H), 3.30 (d, *J* = 10.0 Hz, 1H), 1.87–1.83 (m, 1H), 1.62 (d, *J* = 10.0 Hz, 1H), 1.55–1.45 (m, 2H), 1.39–

1.34 (m, 2H), 1.22 (s, 1H), 1.17 (s, 3H), 1.09 (s, 3H), 0.99 (d, $J = 10.0$ Hz, 3H). HRMS (ESI+) m/z calcd [C₂₇H₃₂FN₂O₂] [(M + H)]⁺ 435.2448, found 435.2442.

4.1.1 General procedure for the synthesis of compounds 8a-l.—To a solution of iodo derivatives (**3a**, **3b** and **3c**, 1.0 mmol, 1 equiv) and boronic acids or esters (**7**, 1.5 mmol, 1.5 equiv) in 1,4-dioxane (4.0 mL) was added 1.0 mL of water. The reaction mixture was degassed with argon for about 30 minutes. After that Pd(dppf)Cl₂.DCM (0.05 equiv, 0.05 mmol) and Na₂CO₃ (2 equiv, 2.0 mmol) were added to the reaction mixture and again degassed with argon for another 20 minutes. The reaction mixture was stirred under reflux for 3 h. After cooled down to room temperature, the mixture was extracted with EtOAc, washed with brine, dried over Na₂SO₄, and concentrated under reduced pressure. The crude product was purified by column chromatography (Silica, Hexane/EtOAc = 1:9 for **8a-b**, **8h-j** and **8l**, Hexane/EtOAc = 7:3 for **8g** and **8k** and CH₂Cl₂/MeOH = 9:1 for **8c-f**) (see Scheme 3).

(4-(6Fluoropyridin-3-yl)-3-methoxyphenyl)(1,3,3-trimethyl-6-azabicyclo[3.2.1]octan-6yl)methanone (8a): To afford yellow solid (0.072 g, 78.2%). ¹H NMR (500 MHz, CDCl₃) δ 8.36 (s, 1H), 7.99 (t, $J = 10.0$ Hz, 1H), 7.33 (t, $J = 10.0$ Hz, 1H), 7.15–7.10 (m, 2H), 7.00 (d, $J = 10.0$ Hz, 1H), 4.66 (s, 1H), 3.87 (s, 3H), 3.63 (d, $J = 10.0$ Hz, 1H), 3.35 (t, $J = 10.0$ Hz, 1H), 1.84–1.81 (m, 1H), 1.68–1.62 (m, 2H), 1.56–1.48 (m, 2H), 1.40–1.38 (m, 1H), 1.29 (d, $J = 10.0$ Hz, 1H), 1.18 (s, 3H), 1.10 (s, 3H), 0.98 (d, $J = 10.0$ Hz, 3H). HRMS (ESI+) m/z calcd [C₂₃H₂₈FN₂O₂] [(M + H)]⁺ 383.2135, found 383.2129.

(4-(2Fluoropyridin-3-yl)-3-methoxyphenyl)(1,3,3-trimethyl-6-azabicyclo[3.2.1]octan-6yl)methanone (8b): To afford yellow solid (0.075 g, 81.5%). ¹H NMR (500 MHz, CDCl₃) δ 8.21 (s, 1H), 7.79 (t, $J = 10.0$ Hz, 1H), 7.31–7.24 (m, 2H), 7.11–7.06 (m, 2H), 4.64 (s, 1H), 3.84 (s, 3H), 3.61 (d, $J = 10.0$ Hz, 1H), 3.33 (t, $J = 10.0$ Hz, 1H), 1.80–1.78 (m, 1H), 1.68–1.62 (m, 1H), 1.54–1.44 (m, 2H), 1.40–1.34 (m, 2H), 1.28 (d, $J = 10.0$ Hz, 1H), 1.16 (s, 3H), 1.08 (s, 3H), 0.96 (d, $J = 10.0$ Hz, 3H). HRMS (ESI+) m/z calcd [C₂₃H₂₈FN₂O₂] [(M + H)]⁺ 383.2135, found 383.2129.

(3Methoxy-4-(1-methyl-1H-indol-3-yl)phenyl)(1,3,3-trimethyl-6-azabicyclo[3.2.1]octan-6yl)methanone (8c): To afford yellow solid (0.082 g, 82.0%). ¹H NMR (500 MHz, CDCl₃) δ 7.82 (d, $J = 10.0$ Hz, 1H), 7.68 (d, $J = 10.0$ Hz, 1H), 7.47 (s, 1H), 7.38 (d, $J = 5.0$ Hz, 1H), 7.19–7.14 (m, 3H), 4.69 (s, 1H), 3.92 (s, 3H), 3.88 (s, 3H), 3.85 (d, $J = 10.0$ Hz, 1H), 3.65 (d, $J = 10.0$ Hz, 1H), 3.39–3.32 (m, 1H), 1.89–1.84 (m, 2H), 1.79–1.76 (m, 1H), 1.57–1.47 (m, 1H), 1.43–1.41 (m, 1H), 1.35 (d, $J = 10.0$ Hz, 1H), 1.19 (s, 3H), 1.11 (s, 3H), 0.98 (d, $J = 10.0$ Hz, 3H). HRMS (ESI+) m/z calcd [C₂₇H₃₃N₂O₂] [(M + H)]⁺ 417.2542, found 417.2540.

(3Methoxy-4-(1H-pyrrolo[2,3-b]pyridin-3-yl)phenyl)(1,3,3-trimethyl-6-azabicyclo[3.2.1]octan-6yl)methanone (8d): To afford yellow solid (0.05 g, 51.5%). ¹H NMR (500 MHz, CDCl₃) δ 8.31 (s, 1H), 8.23 (d, $J = 10.0$ Hz, 1H), 7.70 (s, 1H), 7.55 (t, $J = 5.0$ Hz, 1H), 7.23 (t, $J = 5.0$ Hz, 1H), 7.16–7.12 (m, 2H), 4.66 (s, 1H), 3.89 (s, 3H), 3.62 (d, $J = 10.0$ Hz, 1H), 3.40–3.33 (m, 1H), 2.16 (s, 1H), 1.82–1.70 (m, 2H), 1.63–1.58 (m, 1H), 1.51–1.44 (m, 1H), 1.40–1.34 (m, 2H), 1.29 (d, $J = 10.0$ Hz, 1H), 1.16 (s, 3H), 1.10 (s, 3H),

0.98 (d, $J = 10.0$ Hz, 3H). HRMS (ESI+) m/z calcd [$C_{25}H_{30}N_3O_2$] [(M + H)]⁺ 404.2338, found 404.2330.

(3Methoxy-4-(1H-pyrrolo[2,3-c]pyridin-3-yl)phenyl)(1,3,3-trimethyl-6-aza-bicyclo[3.2.1]octan-6-yl)methanone (8e): To afford pale yellow solid (0.056 g, 57.7%). ¹H NMR (500 MHz, CDCl₃) δ 8.31 (s, 1H), 8.23 (d, $J = 10.0$ Hz, 1H), 7.72 (s, 1H), 7.56 (t, $J = 5.0$ Hz, 1H), 7.25 (t, $J = 5.0$ Hz, 1H), 7.16–7.12 (m, 2H), 4.66 (s, 1H), 3.89 (s, 3H), 3.62 (d, $J = 10.0$ Hz, 1H), 3.40–3.33 (m, 1H), 2.16 (s, 1H), 1.82–1.70 (m, 2H), 1.63–1.58 (m, 1H), 1.51–1.44 (m, 1H), 1.40–1.34 (m, 2H), 1.28 (d, $J = 10.0$ Hz, 1H), 1.16 (s, 3H), 1.10 (s, 3H), 0.98 (d, $J = 10.0$ Hz, 3H). HRMS (ESI+) m/z calcd [$C_{25}H_{30}N_3O_2$] [(M + H)]⁺ 404.2338, found 404.2330.

(3Methoxy-4-(1H-pyrrolo[3,2-c]pyridin-3-yl)phenyl)(1,3,3-trimethyl-6-aza-bicyclo[3.2.1]octan-6-yl)methanone (8f): To afford yellow solid (0.048 g, 49.4%). ¹H NMR (500 MHz, MeOD) δ 8.32 (s, 1H), 8.27 (d, $J = 10.0$ Hz, 1H), 7.78 (d, $J = 5.0$ Hz, 1H), 7.68 (t, $J = 5.0$ Hz, 1H), 7.27 (t, $J = 5.0$ Hz, 1H), 7.20 (d, $J = 5.0$ Hz, 1H), 7.17–7.15 (m, 1H), 4.57 (s, 1H), 3.92 (s, 3H), 3.62 (d, $J = 10.0$ Hz, 1H), 3.28–3.26 (m, 1H), 1.92–1.87 (m, 1H), 1.70–1.61 (m, 2H), 1.56–1.49 (m, 1H), 1.43–1.41 (m, 2H), 1.35 (d, $J = 10.0$ Hz, 1H), 1.18 (s, 3H), 1.10 (s, 3H), 0.98 (d, $J = 10.0$ Hz, 3H). HRMS (ESI+) m/z calcd [$C_{25}H_{30}N_3O_2$] [(M + H)]⁺ 404.2338, found 404.2330.

(2'-Methylbiphenyl-4-yl)(1,3,3-trimethyl-6-aza-bicyclo[3.2.1]octan-6-yl)methanone (8g): To afford colorless semi solid (0.07 g, 77.8%). ¹H NMR (500 MHz, CDCl₃) δ 7.53 (t, $J = 10.0$ Hz, 2H), 7.37 (d, $J = 10.0$ Hz, 2H), 7.30–7.28 (m, 2H), 7.24 (d, $J = 10.0$ Hz, 2H), 4.68 (s, 1H), 3.65 (d, $J = 10.0$ Hz, 1H), 3.39–3.34 (m, 1H), 2.29 (s, 1H), 1.84–1.79 (m, 1H), 1.70–1.62 (m, 1H), 1.56–1.46 (m, 2H), 1.42–1.36 (m, 2H), 1.28 (d, $J = 10.0$ Hz, 1H), 1.19 (s, 3H), 1.10 (s, 3H), 0.98 (d, $J = 10.0$ Hz, 3H). HRMS (ESI+) m/z calcd [$C_{24}H_{30}NO$] [(M + H)]⁺ 348.2327, found 348.2320.

(4-(3-Methylpyridin-4-yl)phenyl)(1,3,3-trimethyl-6-aza-bicyclo[3.2.1]octan-6-yl)methanone (8h): To afford pale yellow solid (0.072 g, 80.0%). ¹H NMR (500 MHz, CDCl₃) δ 8.52 (s, 1H), 8.48 (t, $J = 5.0$ Hz, 1H), 7.56–7.53 (m, 2H), 7.38–7.35 (s, 2H), 7.14 (t, $J = 5.0$ Hz, 1H), 4.65 (s, 1H), 3.64 (d, $J = 10.0$ Hz, 1H), 3.34–3.32 (m, 1H), 2.28 (s, 3H), 1.81–1.76 (m, 2H), 1.64–1.51 (m, 1H), 1.49–1.46 (m, 1H), 1.38–1.34 (m, 2H), 1.28 (d, $J = 10.0$ Hz, 1H), 1.16 (s, 3H), 1.08 (s, 3H), 0.97 (d, $J = 10.0$ Hz, 3H). HRMS (ESI+) m/z calcd [$C_{24}H_{29}N_2O$] [(M + H)]⁺ 349.2280, found 349.2274.

(4-(4-Methylpyridin-3-yl)phenyl)(1,3,3-trimethyl-6-aza-bicyclo[3.2.1]octan-6-yl)methanone (8i): To afford pale yellow solid (0.075 g, 83.3%). ¹H NMR (500 MHz, CDCl₃) δ 8.48 (t, $J = 10.0$ Hz, 2H), 7.57 (t, $J = 5.0$ Hz, 2H), 7.39–7.36 (m, 2H), 7.29 (s, 1H), 4.67 (s, 1H), 3.65 (d, $J = 10.0$ Hz, 1H), 3.37–3.33 (m, 1H), 2.28 (s, 3H), 1.84–1.81 (m, 1H), 1.67–1.62 (m, 1H), 1.50–1.42 (m, 2H), 1.41–1.38 (m, 2H), 1.28 (d, $J = 10.0$ Hz, 1H), 1.19 (s, 3H), 1.10 (s, 3H), 0.98 (d, $J = 10.0$ Hz, 3H). HRMS (ESI+) m/z calcd [$C_{24}H_{29}N_2O$] [(M + H)]⁺ 349.2280, found 349.2274.

(4-(2-Methylpyridin-3-yl)phenyl)(1,3,3-trimethyl-6-aza-bicyclo[3.2.1]octan-6-yl)methanone (8j): To afford pale yellow solid (0.069 g, 76.6%). ¹H NMR (500 MHz, CDCl₃) δ 8.52 (d, *J* = 5.0 Hz, 1H), 7.55–7.50 (m, 3H), 7.37–7.34 (m, 2H), 7.20 (t, *J* = 5.0 Hz, 1H), 4.65 (s, 1H), 3.64 (d, *J* = 10.0 Hz, 1H), 3.35–3.31 (m, 1H), 2.51 (s, 3H), 1.82–1.78 (m, 1H), 1.65–1.60 (m, 1H), 1.54–1.44 (m, 2H), 1.40–1.34 (m, 2H), 1.25 (d, *J* = 10.0 Hz, 1H), 1.16 (s, 3H), 1.08 (s, 3H), 0.97 (d, *J* = 10.0 Hz, 3H). HRMS (ESI+) *m/z* calcd [C₂₄H₂₉N₂O] [(M + H)]⁺ 349.2280, found 349.2274.

(3-Fluoro-6'-methylbiphenyl-4-yl)(1,3,3-trimethyl-6-aza-bicyclo[3.2.1]octan-6-yl)methanone (8k): To afford white yellow solid (0.072 g, 79.1%). ¹H NMR (500 MHz, CDCl₃) δ 7.40–7.35 (m, 1H), 7.31–7.28 (m, 2H), 7.25–7.23 (m, 1H), 7.21–7.19 (m, 1H), 7.16–7.13 (m, 1H), 7.08–7.04 (m, 1H), 4.66 (s, 1H), 3.65 (d, *J* = 10.0 Hz, 1H), 3.31–3.29 (m, 1H), 2.28 (s, 3H), 1.84–1.81 (m, 1H), 1.62–1.58 (m, 1H), 1.50–1.42 (m, 2H), 1.41–1.38 (m, 2H), 1.28 (d, *J* = 10.0 Hz, 1H), 1.15 (s, 3H), 1.06 (s, 3H), 0.94 (d, *J* = 10.0 Hz, 3H). HRMS (ESI+) *m/z* calcd [C₂₄H₂₉FNO] [(M + H)]⁺ 366.2233, found 366.2228.

(2Fluoro-4-(4-methylpyridin-3-yl)phenyl)(1,3,3-trimethyl-6-aza-bicyclo[3.2.1]octan-6-yl)methanone (8l): To afford yellow solid (0.075 g, 82.4%). ¹H NMR (500 MHz, CDCl₃) δ 8.48 (d, *J* = 5.0 Hz, 1H), 8.43 (d, *J* = 5.0 Hz, 1H), 7.46–7.41 (m, 1H), 7.21 (d, *J* = 5.0 Hz, 1H), 7.17–7.15 (m, 1H), 7.10–7.06 (m, 1H), 4.66 (s, 1H), 3.66 (d, *J* = 10.0 Hz, 1H), 3.31–3.29 (m, 1H), 2.30 (s, 3H), 1.87–1.78 (m, 1H), 1.62–1.59 (m, 1H), 1.55–1.47 (m, 2H), 1.44–1.35 (m, 2H), 1.23 (d, *J* = 10.0 Hz, 1H), 1.15 (s, 3H), 1.09 (s, 3H), 0.94 (d, *J* = 10.0 Hz, 3H). HRMS (ESI+) *m/z* calcd [C₂₃H₂₈FN₂O] [(M + H)]⁺ 367.2186, found 367.2180.

***Tert*-butyl 3-(2-methoxy-4-(methoxycarbonyl)phenyl)-1H-indole-1-carboxylate (10):** To a solution of methyl 4-iodo-3-methoxybenzoate (**9**) (0.5 g, 1.71 mmol) and *tert*-butyl 3-(4,4,5,5-tetramethyl-1,3,2-dioxaborolan-2-yl)-1H-indole-1-carboxylate (0.70 g, 2.05 mmol) in 1,4-dioxane (10.0 mL) was added 2.0 mL of water. The reaction mixture was degassed with argon for about 30 minutes. After that Pd(dppf)Cl₂.DCM (0.069 g, 0.085 mmol) and Na₂CO₃ (0.36 g, 3.42 mmol) were added to the reaction mixture and again degassed with argon for another 20 minutes. The reaction mixture was stirred under reflux for 3 h. After cooled down to room temperature, the mixture was extracted with EtOAc, washed with brine, dried over Na₂SO₄, and concentrated under reduced pressure. The crude product was purified by column chromatography (Hexane/EtOAc = 4:6) to afford **10** as a yellow solid (0.52 g, 79.7%). ¹H NMR (500 MHz, CDCl₃) δ 8.15 (d, *J* = 5.0 Hz, 1H), 7.85 (s, 1H), 7.65 (d, *J* = 10.0 Hz, 2H), 7.56 (d, *J* = 10.0 Hz, 2H), 7.32 (d, *J* = 10.0 Hz, 1H), 7.28 (s, 1H), 3.86 (s, 3H), 3.82 (s, 3H), 1.62 (s, 9H).

Methyl 4-(1H-indol-3-yl)-3-methoxybenzoate (11): To a solution of *tert*-butyl 3-(2-methoxy-4-(methoxycarbonyl)phenyl)-1H-indole-1-carboxylate (**10**) (0.5 g, 1.31 mmol) in methylene chloride (25 mL) was added trifluoroacetic acid (0.4 mL, 5.24 mmol) dropwise at 0 °C, and then, the mixture was stirred at room temperature for 8 h. After completion of the reaction, the reaction mixture was concentrated under reduced pressure. The resulting residue was purified by silica gel column chromatography (Hexane:EtOAc = 2:8) to give **11**

as a yellow solid (0.32 g, 86.9% yield). $^1\text{H NMR}$ (500 MHz, CDCl_3) δ 8.38 (s, 1H), 7.85 (d, $J = 5.0$ Hz, 1H), 7.78 (s, 2H), 7.70 (d, $J = 10.0$ Hz, 2H), 7.47 (d, $J = 5.0$ Hz, 1H), 7.28 (d, $J = 10.0$ Hz, 1H), 7.22 (d, $J = 5.0$ Hz, 1H), 3.98 (s, 3H), 3.96 (s, 3H).

4-(1H-Indol-3-yl)-3-methoxybenzoic acid (12): A solution of methyl 4-(1H-indol-3-yl)-3-methoxybenzoate (**11**) (0.3 g, 1.06 mmol) in THF/H₂O (3:1 3 mL) was treated with lithium hydroxide monohydrate (0.22 g, 5.33 mmol) and stirred at room temperature for overnight. The reaction mixture was then acidified with 10% HCl to pH 4 and then partitioned between EtOAc and brine. The organic layer was separated, dried over anhydrous MgSO_4 , filtered, and concentrated *in vacuo*. The resulting residue was purified by silica gel column chromatography (CH_2Cl_2 :MeOH = 9:1) to give 4-(4-methoxybenzyloxy)-3-nitrobenzoic acid as a pale yellow solid (0.25 g, 87.7% yield). $^1\text{H NMR}$ (500 MHz, $\text{DMSO}-d_6$) δ 11.44 (s, 1H), 7.74–7.70 (m, 3H), 7.64 (d, $J = 10.0$ Hz, 1H), 7.60 (s, 1H), 7.46 (d, $J = 10.0$ Hz, 1H), 7.16–7.13 (m, 1H), 7.08 (t, $J = 5.0$ Hz, 1H).

(4-(1H-Indol-3-yl)-3-methoxyphenyl)(4-methylpiperazin-1-yl)methanone (13a): To the mixture of 4-(1H-indol-3-yl)-3-methoxybenzoic acid (**12**) (0.04 g, 0.15 mmol), 1-methyl piperazine (0.018 g, 0.18 mmol), EDC.HCl (0.034 g, 0.18 mmol), and HOBT (0.024 g, 0.18 mmol), in DMF (10 mL) was added DIPA (0.05 mL, 0.30 mmol). The reaction mixture was stirred at room temperature overnight and then partitioned between EtOAc and brine. The organic layer was separated, dried over anhydrous MgSO_4 , filtered, and concentrated under a vacuum. The resulting residue was purified by silica gel column chromatography (CH_2Cl_2 :MeOH = 9:1) to give **13a** as a white solid (0.031 g, 59.6% yield). $^1\text{H NMR}$ (500 MHz, CDCl_3) δ 8.39 (s, 1H), 7.78 (d, $J = 5.0$ Hz, 1H), 7.54 (d, $J = 5.0$ Hz, 1H), 7.43 (d, $J = 5.0$ Hz, 1H), 7.23–7.18 (m, 1H), 7.17–7.14 (m, 1H), 7.10 (d, $J = 5.0$ Hz, 1H), 7.06 (d, $J = 5.0$ Hz, 1H), 3.87 (s, 3H), 3.83–3.60 (m, 4H), 2.50–2.46 (m, 4H), 2.35 (s, 3H); HRMS (ESI+) m/z calcd [$\text{C}_{21}\text{H}_{24}\text{N}_3\text{O}_2$] [(M + H)]⁺ 350.1869, found 350.1863.

(4-(1H-Indol-3-yl)-3-methoxyphenyl)(4,4-difluoropiperidin-1-yl)methanone (13b): To the mixture of 4-(1H-indol-3-yl)-3-methoxybenzoic acid (**12**) (0.04 g, 0.15 mmol), 4,4-difluoropiperidine hydrochloride (0.028 g, 0.18 mmol), EDC.HCl (0.034 g, 0.18 mmol), and HOBT (0.024 g, 0.18 mmol), in DMF (10 mL) was added DIPA (0.05 mL, 0.30 mmol). The reaction mixture was stirred at room temperature overnight and then partitioned between EtOAc and brine. The organic layer was separated, dried over anhydrous MgSO_4 , filtered, and concentrated under a vacuum. The resulting residue was purified by silica gel column chromatography (CH_2Cl_2 :MeOH = 9:1) to give **13b** as a white solid (0.028 g, 50.9% yield). $^1\text{H NMR}$ (500 MHz, CDCl_3) δ 8.33 (s, 1H), 7.78 (d, $J = 10.0$ Hz, 1H), 7.68 (d, $J = 10.0$ Hz, 1H), 7.57 (d, $J = 5.0$ Hz, 1H), 7.44 (d, $J = 10.0$ Hz, 1H), 7.24 (d, $J = 5.0$ Hz, 1H), 7.19–7.18 (m, 1H), 7.11 (m, 1H), 7.07 (d, $J = 10.0$ Hz, 1H), 3.89 (s, 3H), 3.87–3.80 (m, 4H), 2.06–2.04 (m, 4H); HRMS (ESI+) m/z calcd [$\text{C}_{21}\text{H}_{21}\text{F}_2\text{N}_2\text{O}_2$] [(M + H)]⁺ 371.1571, found 371.1566.

(4-(1H-Indol-3-yl)-3-methoxyphenyl)(4-methyl-1,4-diazepan-1-yl)methanone (13c): To the mixture of 4-(1H-indol-3-yl)-3-methoxybenzoic acid (**12**) (0.04 g, 0.15 mmol), 1-methyl-1,4-diazepane (0.02 g, 0.18 mmol), EDC.HCl (0.034 g, 0.18 mmol), and

HOBT (0.024 g, 0.18 mmol), in DMF (10 mL) was added DIPA (0.05 mL, 0.30 mmol). The reaction mixture was stirred at room temperature overnight and then partitioned between EtOAc and brine. The organic layer was separated, dried over anhydrous MgSO₄, filtered, and concentrated under a vacuum. The resulting residue was purified by silica gel column chromatography (CH₂Cl₂:MeOH = 9:1) to give **12c** as a white solid (0.034 g, 62.9% yield). ¹H NMR (500 MHz, CDCl₃) δ 8.42 (s, 1H), 7.78 (d, *J* = 5.0 Hz, 1H), 7.65 (d, *J* = 5.0 Hz, 1H), 7.53 (d, *J* = 5.0 Hz, 1H), 7.42 (d, *J* = 5.0 Hz, 1H), 7.27–7.22 (m, 1H), 7.18–7.15 (m, 1H), 7.08–7.05 (m, 2H), 3.86 (s, 3H), 3.83–3.81 (m, 2H), 3.66 (t, *J* = 5.0 Hz, 1H), 3.60 (t, *J* = 5.0 Hz, 1H), 2.79 (t, *J* = 5.0 Hz, 1H), 2.68 (t, *J* = 5.0 Hz, 1H), 2.63–2.60 (m, 2H), 2.42 (s, 3H), 2.04 (t, *J* = 5.0 Hz, 1H), 1.91 (t, *J* = 5.0 Hz, 1H); HRMS (ESI+) *m/z* calcd [C₂₂H₂₆N₃O₂] [(M + H)⁺] 364.2025, found 364.2020.

N-Adamantan-1-yl-4-(1H-indol-3-yl)-3-methoxybenzamide (13d): To the mixture of 4-(1H-indol-3-yl)-3-methoxybenzoic acid (**12**) (0.04 g, 0.15 mmol), 1-Adamantylamine (0.027 g, 0.18 mmol), EDC.HCl (0.034 g, 0.18 mmol), and HOBT (0.024 g, 0.18 mmol), in DMF (10 mL) was added DIPA (0.05 mL, 0.30 mmol). The reaction mixture was stirred at room temperature overnight and then partitioned between EtOAc and brine. The organic layer was separated, dried over anhydrous MgSO₄, filtered, and concentrated under a vacuum. The resulting residue was purified by silica gel column chromatography (Hexane:EtOAc = 7:3) to give **13d** as a white solid (0.03 g, 50.8% yield). ¹H NMR (500 MHz, CDCl₃) δ 8.37 (s, 1H), 7.78 (d, *J* = 5.0 Hz, 1H), 7.67 (d, *J* = 5.0 Hz, 1H), 7.60 (d, *J* = 5.0 Hz, 1H), 7.55 (d, *J* = 5.0 Hz, 1H), 7.43 (d, *J* = 5.0 Hz, 1H), 7.28–7.22 (m, 2H), 7.19–7.16 (m, 1H), 5.90 (s, 1H), 3.92 (s, 3H), 2.18–2.16 (m, 9H), 1.78–1.72 (m, 6H); HRMS (ESI+) *m/z* calcd [C₂₆H₂₉N₂O₂] [(M + H)⁺] 401.2229, found 401.2224.

N-(4-Fluorophenyl)-4-(1H-indol-3-yl)-3-methoxybenzamide (13e): To the mixture of 4-(1H-indol-3-yl)-3-methoxybenzoic acid (**12**) (0.04 g, 0.15 mmol), 4-fluorobenzylamine (0.02 g, 0.164 mmol), EDC.HCl (0.034 g, 0.18 mmol), and HOBT (0.024 g, 0.18 mmol), in DMF (10 mL) was added DIPA (0.05 mL, 0.30 mmol). The reaction mixture was stirred at room temperature overnight and then partitioned between EtOAc and brine. The organic layer was separated, dried over anhydrous MgSO₄, filtered, and concentrated under a vacuum. The resulting residue was purified by silica gel column chromatography (Hexane:EtOAc = 6:4) to give **13e** as a brown solid (0.02 g, 37.7% yield). ¹H NMR (500 MHz, CDCl₃) δ 8.38 (s, 1H), 7.86–7.77 (m, 3H), 7.66–7.64 (m, 4H), 7.46 (d, *J* = 10.0 Hz, 2H), 7.27 (d, *J* = 10.0 Hz, 1H), 7.22–7.19 (m, 1H), 7.11–7.08 (m, 2H), 3.96 (s, 3H); HRMS (ESI+) *m/z* calcd [C₂₂H₁₈FN₂O₂] [(M + H)⁺] 361.1352, found 361.1350.

4.1.2. Chiral HPLC separation of compound 1 and 6a.—Racemic **1** was separated into two enantiomers (1*S*,5*R*)-**1** (*t_R* 10.9 min; ee 98%) and (1*R*,5*S*)-**1** (*t_R* 13.9 min; ee 97%) by preparative chiral HPLC. Method: Chiralcel OD, 10×250 mm; mobile phase: hexane/2propanol 90/10; 8 mL/min; UV 254 nm. The chiral structure of the enantiomers that was determined previously²² was confirmed here by the V_{1a} binding assay as described below. The enantiomeric purity of [¹¹C](1*S*,5*R*)-**1** (e.e.>95%) was tested under the same HPLC conditions.

Racemic compound **6a** was separated into two enantiomers (*1S,5R*)-**6a** ($t_R = 3.5$ min; ee 99.5%) and (*1R,5S*)-**6a** ($t_R \sim 6$ min; ee 99.1%) by preparative supercritical fluid chromatography (SFC) commercially (Averica, Marlborough, MA). Method: column: 2.1×25.0 cm Chiralpak AD-H from Chiral Technologies (West Chester, PA); CO₂ co-solvent – ethanol; isocratic method: 50% co-solvent at 60 g/min; pressure: 85 bar, temperature: 25°C.

4.2. *In vitro* binding assay

of all vasopressin compounds was performed commercially by Eurofins CEREP (Celle L'Evescault, France) (assay number 0159) as described elsewhere [37]. Briefly, the assay conditions are shown in the Table below. Nonspecific binding was defined as that remaining in the presence of 1 μ M AVP.

Receptor	Source	Radiotracer	Conc.	K _D	Incubation
(h)V _{1a}	Human recombinant (CHO cells)	[³ H]AVP	0.3 nM	0.5 nM	60 min, RT

The assays were done two times independently, each in duplicate, at selected concentrations of the test compounds. The binding assay results were analyzed using a one-site competition model, and IC₅₀ curves were generated based on a sigmoidal dose response with variable slope. The K_i values were calculated using the Cheng–Prusoff equation.

4.3. Radiochemistry

[¹¹C]iodomethane was prepared with the General Electric TRACERlab FX MeI (GE, Milwaukee, WI) using a GE PETtrace cyclotron.

4.3.1. Radiosynthesis of [¹¹CH₃](*1S,5R*)-1****—A solution of 1 mg precursor (*1S,5R*)-**6a** ((3-hydroxy-4-(1H-indol-3-yl)phenyl)(1,3,3-trimethyl-6azabicyclo[3.2.1]octan-6-yl)methanone) in 0.2 mL DMSO was placed in a 1 mL V-vial and 1.0 mg K₂CO₃ was added. The mixture was sonicated for 5 min. [¹¹C]iodomethane, carried by a stream of nitrogen, was trapped in the above solution of the precursor. The reaction was heated in an 80 °C water bath for 3.5 min, then quenched with 0.2 mL of water. The crude reaction product was purified by reverse-phase HPLC (column: Waters XBridge C18, 10 μ , 10 \times 250 mm; mobile phase: acetonitrile/water/triethylamine 580/420/2; flow rate: 10 mL/min; UV: 254 nm). The radioactive peak ($t_R = 6.5$ min) that was separated from the precursor ($t_R = 3.1$ min) was collected in solution of 0.25 g ascorbic acid and 60 mL water. The water solution was passed through an activated Waters C-18 Oasis HLB light solid-phase extraction (SPE) cartridge. After the SPE was washed with 10 mL of saline, the product was eluted with ethanol (1 mL) and diluted with 10 mL saline. The final product solution was analyzed by analytical HPLC (column: Waters Xbridge C18, 10 μ , 250 \times 4.6 mm; mobile phase acetonitrile/water/triethylamine 70/30/1; flow rate: 3 ml/min; UV 254 nm). A single radioactive peak ($t_R = 3.2$ min) corresponding to [¹¹CH₃](*1S,5R*)-**1** was observed. The specific radioactivity at the end-of-synthesis was calculated by relating radioactivity to the mass associated with the UV absorbance peak of carrier.

4.4. Animal studies.

Baseline study in CD1 mice: Male, CD-1 mice weighing 25–27 g from Charles River (Wilmington, MA) were used. The animals were sacrificed by cervical dislocation at 5, 15, 30 and 60 min following injection of 3.7 MBq (0.1 mCi) [^{11}C](1*S*,5*R*)-**1** (specific radioactivity = 232 GBq/ μmole (8,600 mCi/ μmol) in 0.2 mL saline into a lateral tail vein ($n = 3$). The brains were removed and dissected on ice. Septum, cortex, hippocampus, and the rest of brain were weighed and their radioactivity content was determined in a γ -counter LKB/Wallac 1283 CompuGamma CS (Perkin Elmer, Bridgeport, CT). Aliquots of the injectate were prepared as standards and their radioactivity content was determined along with the tissue samples. The percent of injected dose per gram of tissue (%ID/g tissue) was calculated.

Blocking of [^{11}C](1*S*,5*R*)-1** binding in CD1 mice:** *In vivo* binding specificity (blocking) studies were carried out by subcutaneous (SC) administration of various doses (0 mg/kg, 0.3 mg/kg, 1 mg/kg, 3 mg/kg) of ligand **8g** followed by IV injection of 3.7 MBq (0.1 mCi) [^{11}C](1*S*,5*R*)-**1** 30 min thereafter ($n = 3$). Thirty minutes after administration of the radiotracer the animals were sacrificed by cervical dislocation, brain tissues were harvested, and their radioactivity content was determined.

4.4.1. Effect of anesthetics on the [^{11}C](1*S*,5*R*)-1** binding in CD1 mice:** The study was performed similarly to the blocking experiments with CD1 mice. All anesthetics were injected ip (80 mg/kg), 30 min prior the radiotracer.

4.4.2. Brain regional distribution of [^{11}C](1*S*,5*R*)-1** in prairie voles:** male, prairie voles weighing 47–58 g from Kinsey Institute Indiana University (Bloomington, IN) were used. The experiments were performed similarly to the experiments with CD1 mice. The radiotracer was injected into retro-orbital venous sinus under a brief isoflurane anesthesia [38].

ACKNOWLEDGMENTS

This research was supported in part by NIH grant R01MH107197 (Wong, Horti), John Davis Foundation grant and Division of Nuclear Medicine and Molecular Imaging. We thank Paige Finley and Polina Sysa Shah for the help with animal experiments and Julia Buchanan for editorial comments.

ABBREVIATIONS

PET	positron emission tomography
ADH	antidiuretic hormone
AVP	arginine vasopressin
DMF	<i>N,N</i> dimethylformamide
DIPEA	<i>N,N</i> -Diisopropylethylamine
HPLC	high-performance liquid chromatography

REFERENCES

- [1]. Ishikawa S, Cellular actions of arginine vasopressin in the kidney, *Endocrine Journal* 40 (1993) 373–386. [PubMed: 7920891]
- [2]. Silva YJ, Moffat RC, Walt AJ, Vasopressin effect on portal and systemic hemodynamics. Studies in intact, unanesthetized humans, *JAMA Journal* 210 (1969) 1065–1068.
- [3]. Johnson ZV, Young LJ, Oxytocin and vasopressin neural networks: Implications for social behavioral diversity and translational neuroscience, *Neuroscience & Biobehavioral Reviews* 76 (2017) 87–98. [PubMed: 28434591]
- [4]. Gobrogge K, Wang Z, The ties that bond: neurochemistry of attachment in voles, *Current Opinion in Neurobiology* 38 (2016) 80–88. [PubMed: 27131991]
- [5]. Winslow JT, Hastings N, Carter CS, Harbaugh CR, Insel TR, A role for central vasopressin in pair bonding in monogamous prairie voles, *Nature* 365 (1993) 545–548. [PubMed: 8413608]
- [6]. Dumais KM, Veenema AH, Vasopressin and oxytocin receptor systems in the brain: Sex differences and sex-specific regulation of social behavior, *Frontiers in Neuroendocrinology* 40 (2016) 1–23. [PubMed: 25951955]
- [7]. Veenema AH, Neumann ID, Central vasopressin and oxytocin release: regulation of complex social behaviours, *Progress in Brain Research* 170 (2008) 261–276. [PubMed: 18655888]
- [8]. Koshimizu TA, Nakamura K, Egashira N, Hiroyama M, Nonoguchi H, Tanoue A, Vasopressin V1a and V1b receptors: from molecules to physiological systems, *Physiological Reviews* 92 (2012) 1813–1864. [PubMed: 23073632]
- [9]. Albers HE, Species, sex and individual differences in the vasotocin/vasopressin system: relationship to neurochemical signaling in the social behavior neural network, *Frontiers in Neuroendocrinology* 36 (2015) 49–71. [PubMed: 25102443]
- [10]. Zhang R, Zhang HF, Han JS, Han SP, Genes Related to Oxytocin and Arginine Vasopressin Pathways: Associations with Autism Spectrum Disorders, *Neuroscience Bulletin* 33 (2017) 238–246. [PubMed: 28283809]
- [11]. Yirmiya N, Rosenberg C, Levi S, Salomon S, Shulman C, Nemanov L, Dina C, Ebstein RP, Association between the arginine vasopressin 1a receptor (AVPR1a) gene and autism in a familybased study: mediation by socialization skills, *Molecular Psychiatry* 11 (2006) 488–494. [PubMed: 16520824]
- [12]. Insel TR, Wang ZX, Ferris CF, Patterns of brain vasopressin receptor distribution associated with social organization in microtine rodents, *The Journal of Neuroscience* 14 (1994) 5381–5392. [PubMed: 8083743]
- [13]. Johnson AE, Audigier S, Rossi F, Jard S, Tribollet E, Barberis C, Localization and characterization of vasopressin binding sites in the rat brain using an iodinated linear AVP antagonist, *Brain Research* 622 (1993) 9–16. [PubMed: 8242389]
- [14]. Young LJ, Toloczko D, Insel TR, Localization of vasopressin (V1a) receptor binding and mRNA in the rhesus monkey brain, *Journal of Neuroendocrinology* 11(1999) 291–297. [PubMed: 10223283]
- [15]. Loup F, Tribollet E, Dubois-Dauphin M, Dreifuss JJ, Localization of high-affinity binding sites for oxytocin and vasopressin in the human brain. An autoradiographic study. *Brain Research* 555 (1991) 220–232. [PubMed: 1657300]
- [16]. Landgraf R, Neumann ID, Vasopressin and oxytocin release within the brain: a dynamic concept of multiple and variable modes of neuropeptide communication, *Frontiers in Neuroendocrinology* 25 (2004) 150–76. [PubMed: 15589267]
- [17]. Heinrichs M, von Dawans B, Domes G, Oxytocin, vasopressin, and human social behavior. *Frontiers in Neuroendocrinology* 30 (2009) 548–557. [PubMed: 19505497]
- [18]. Bielsky IF, Hu SB, Szegda KL, Westphal H, Young LJ, Profound impairment in social recognition and reduction in anxiety-like behavior in vasopressin V1a receptor knockout mice, *Neuropsychopharmacology* 29 (2004) 483–493. [PubMed: 14647484]
- [19]. Egashira N, Tanoue A, Higashihara F, Mishima K, Fukue Y, Takano Y, Tsujimoto G, Iwasaki K, Fujiwara M, V1a receptor knockout mice exhibit impairment of spatial memory in an eight-arm radial maze, *Neuroscience Letters* 356 (2004) 195–198. [PubMed: 15036628]

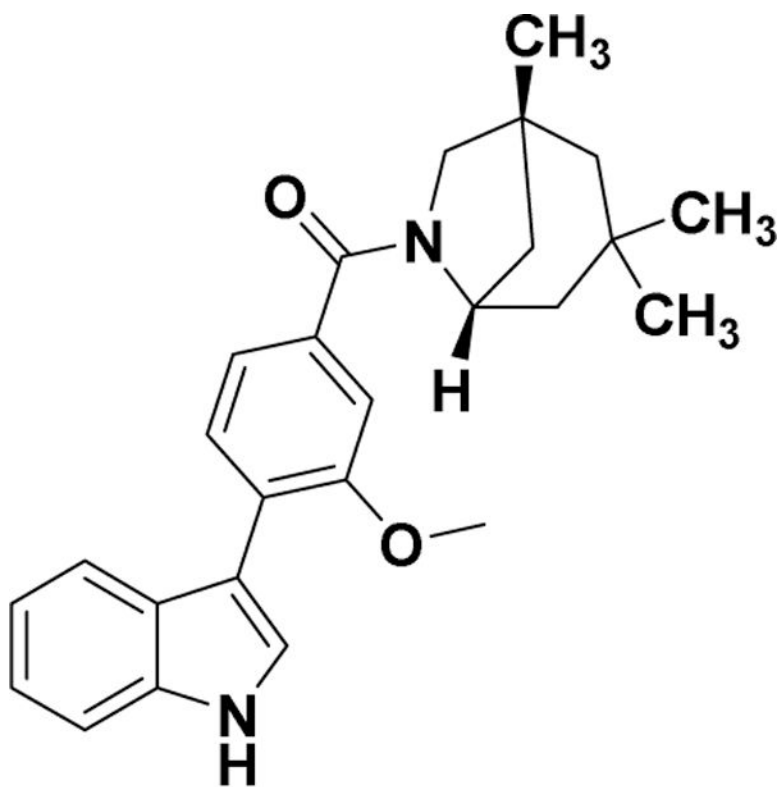
- [20]. Umbricht D, Del Valle Rubido M, Hollander E, McCracken JT, Shic F, Scahill L, Noeideke J, Boak L, Khwaja O, Squassante L, Grundschober C, Kletzl H, Fontoura P, A Single Dose, Randomized, Controlled Proof-Of-Mechanism Study of a Novel Vasopressin 1a Receptor Antagonist (RG7713) in High-Functioning Adults with Autism Spectrum Disorder, *Neuropsychopharmacology* (2016).
- [21]. Fabio K, Guillon C, Lacey CJ, Lu SF, Heindel ND, Ferris CF, Placzek M, Jones G, Brownstein MJ, Simon NG, Synthesis and evaluation of potent and selective human V1a receptor antagonists as potential ligands for PET or SPECT imaging, *Bioorganic & Medicinal Chemistry* 20 (2012) 1337–1345. [PubMed: 22249122]
- [22]. Crombie AL, Antrilli TM, Campbell BA, Crandall DL, Failli AA, He Y, Kern JC, Moore WJ, Nogle LM, Trybulski EJ, Synthesis and evaluation of azabicyclo[3.2.1]octane derivatives as potent mixed vasopressin antagonists, *Bioorganic & Medicinal Chemistry Letters* 20 (2010) 3742–3745. [PubMed: 20471258]
- [23]. Eckelman WC, Reba RC, Gibson RE, Receptor-binding radiotracers: A class of potential radiopharmaceuticals, *Journal of Nuclear Medicine* 20 (1979) 350–357. [PubMed: 43884]
- [24]. Freeman SM, Smith AL, Goodman MM, Bales KL, Selective localization of oxytocin receptors and vasopressin 1a receptors in the human brainstem, *Social Neuroscience* (2016) 1–11.
- [25]. Saito R, Ishiharada N, Ban Y, Honda K, Takano Y, Kamiya H, Vasopressin V1 receptor in rat hippocampus is regulated by adrenocortical functions, *Brain Research* 646 (1994)170–174. [PubMed: 8055336]
- [26]. Szot P, Myers KM, Dorsa DM, Effect of vasopressin administration and deficiency upon 3H-AVP binding sites in the CNS and periphery during development, *Peptides* 13 (1992) 389–394. [PubMed: 1409016]
- [27]. Tribollet E, Barberis C, Jard S, Dubois-Dauphin M, Dreifuss JJ, Localization and pharmacological characterization of high affinity binding sites for vasopressin and oxytocin in the rat brain by light microscopic autoradiography, *Brain Research* 442 (1988) 105–118. [PubMed: 2834008]
- [28]. Szot P, Ferris CF, Dorsa DM, [3H]arginine-vasopressin binding sites in the CNS of the golden hamster, *Neuroscience Letters* 119 (1990) 215–218. [PubMed: 2280896]
- [29]. Waterhouse RN, Determination of lipophilicity and its use as a predictor of blood-brain barrier penetration of molecular imaging agents. *Molecular Imaging Biology* 5 (2003) 376–389. [PubMed: 14667492]
- [30]. Horti AG, Raymont V, Terry GE, In PET and SPECT of Neurobiological Systems Book chapter 11 (2014) 251–319 (Springer).
- [31]. Dubois-Dauphin M, Barberis C, de Bilbao F, Vasopressin receptors in the mouse (*Mus musculus*) brain: sex-related expression in the medial preoptic area and hypothalamus, *Brain Research* 743 (1996) 32–39. [PubMed: 9017227]
- [32]. Chappell AR, Freeman SM, Lin YK, LaPrairie JL, Inoue K, Young LJ, Hayes LD, Distributions of oxytocin and vasopressin 1a receptors in the Taiwan vole and their role in social monogamy, *Journal of Zoology* (1987) 299 (2016) 106–115.
- [33]. Turner LM, Young AR, Rompler H, Schoneberg T, Phelps SM, Hoekstra HE, Monogamy evolves through multiple mechanisms: evidence from V1aR in deer mice, *Molecular Biology and Evolution* 27 (2010) 1269–1278. [PubMed: 20097658]
- [34]. Tanabe K, Kozawa O, Matsuno H, Niwa M, Dohi S, Uematsu T, Effect of propofol on arachidonate cascade by vasopressin in aortic smooth muscle cells: inhibition of PGI2 synthesis, *Anesthesiology* 90 (1999) 215–224. [PubMed: 9915331]
- [35]. Tanaka K, Suzuki M, Sumiyoshi T, Murata M, Tsunoda M, Kurachi M, Subchronic phencyclidine administration alters central vasopressin receptor binding and social interaction in the rat, *Brain Research* 992 (2003) 239–245. [PubMed: 14625062]
- [36]. Le Melleo JM, Baker GB, Neuroactive steroids and anxiety disorders, *Journal of Psychiatry & Neuroscience* 27 (2002) 161–165. [PubMed: 12066445]
- [37]. Tahara A, Saito M, Sugimoto T, Tomura Y, Wada K, Kusayama T, Tsukada J, Ishii N, Yatsu T, Uchida W, Tanaka A, Pharmacological characterization of the human vasopressin receptor

subtypes stably expressed in Chinese hamster ovary cells, *British Journal of Pharmacology* 125 (1998) 1463–1470. [PubMed: 9884074]

- [38]. Yardeni T, Eckhaus M, Morris HD, Huizing M, Hoogstraten-Miller S, Retro-orbital injections in mice, *Lab Animal (NY)* 40 (2011) 155–160.

Highlights

- A series of V_{1a} ligands was prepared for positron-emission tomography (PET).
- A new V_{1a} PET tracer [^{11}C](1*S*,5*R*)-**1** was synthesized and evaluated in rodents.
- [^{11}C](1*S*,5*R*)-**1** specifically labels V_{1a} in the mouse and prairie vole brain.
- The anesthetic Propofol blocks the uptake of [^{11}C](1*S*,5*R*)-**1** in the mouse brain.



(1*S*,5*R*)-1.

Figure 1. Structure of high binding affinity and selective V_{1a} receptor antagonist (1*S*,5*R*)-1.

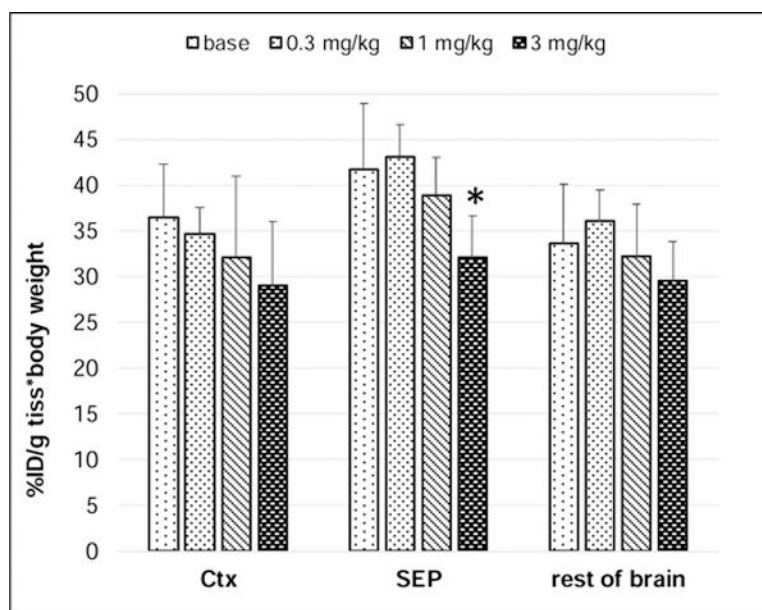


Figure 2. Dose-dependent blocking of $[^{11}\text{CH}_3](1S,5R)\text{-1}$ (0.1 mCi) uptake with the V_{1a} ligand **8g** (subcutaneous blocker) in the CD-1 mouse brain at 30 min after radiotracer injection. Abbreviations: SEP, lateral septum; Ctx, cortex. The blocking study demonstrates that $[^{11}\text{CH}_3](1S,5R)\text{-1}$ specifically (30%) labels V_{1a} in the septum. Data: mean %ID/g tissue \times body weight \pm SD ($n = 3$). * $P = 0.004$, significantly different from baseline (ANOVA).

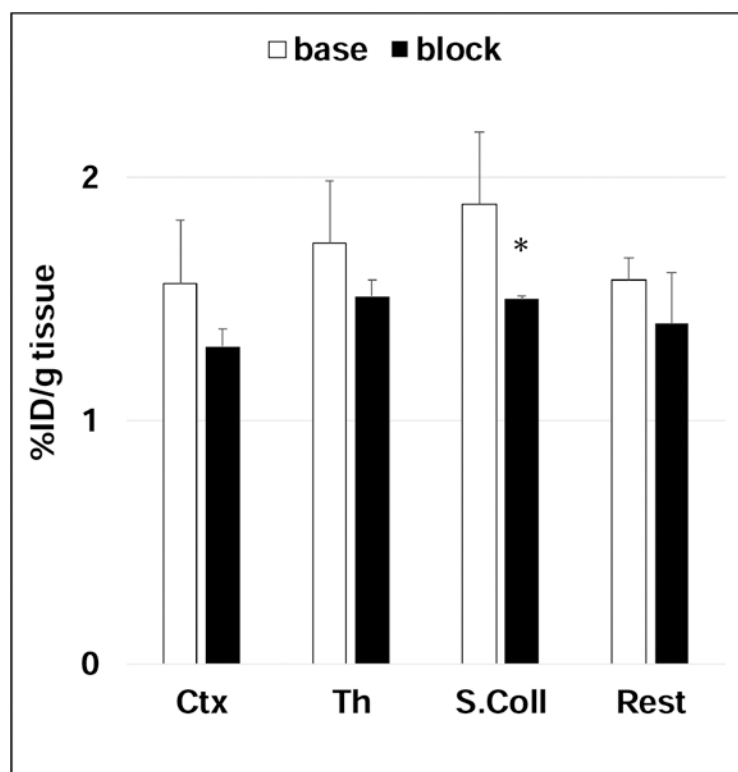


Figure 3.

Brain regional distribution of $[^{11}\text{C}]\text{CH}_3(1S,5R)\text{-1}$ (0.1 mCi) in the baseline and blocking studies in the prairie vole brain at 30 min after radiotracer injection. Blocker is racemic **1** (2 mg/kg). Abbreviations: Ctx, cortex; Th, thalamus; S.Coll, superior colliculus; Rest, the rest of brain. The blocking study demonstrates that $[^{11}\text{C}]\text{CH}_3(1S,5R)\text{-1}$ specifically (34%) labels V_{1a} in the superior colliculus. Data: mean %ID/g tissue \pm SD (n = 6). * $P = 0.01$, significantly different from baseline (ANOVA).

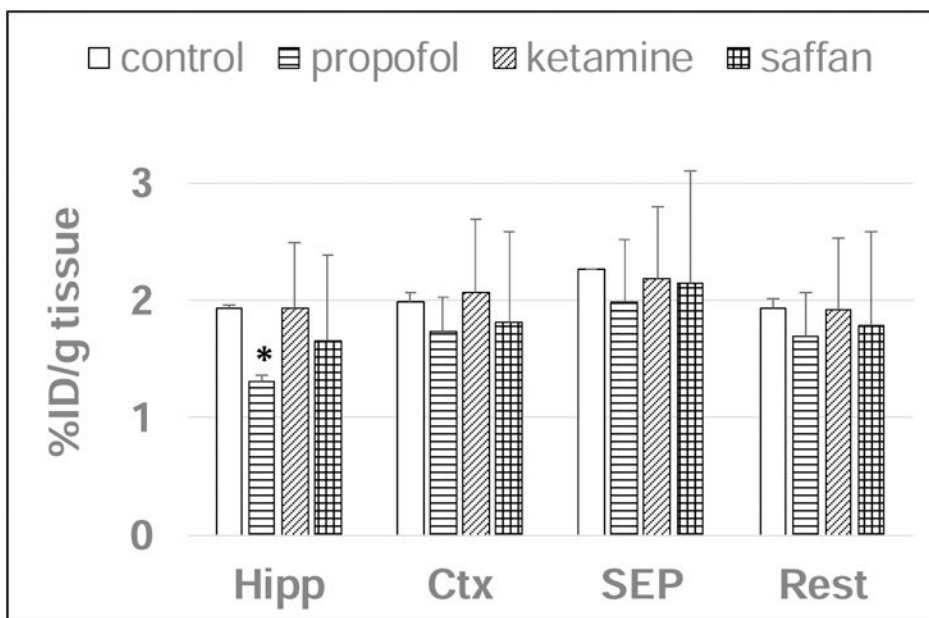
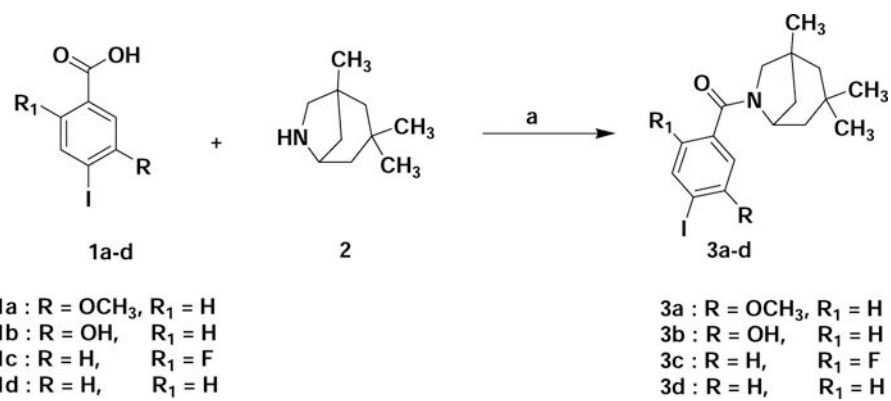
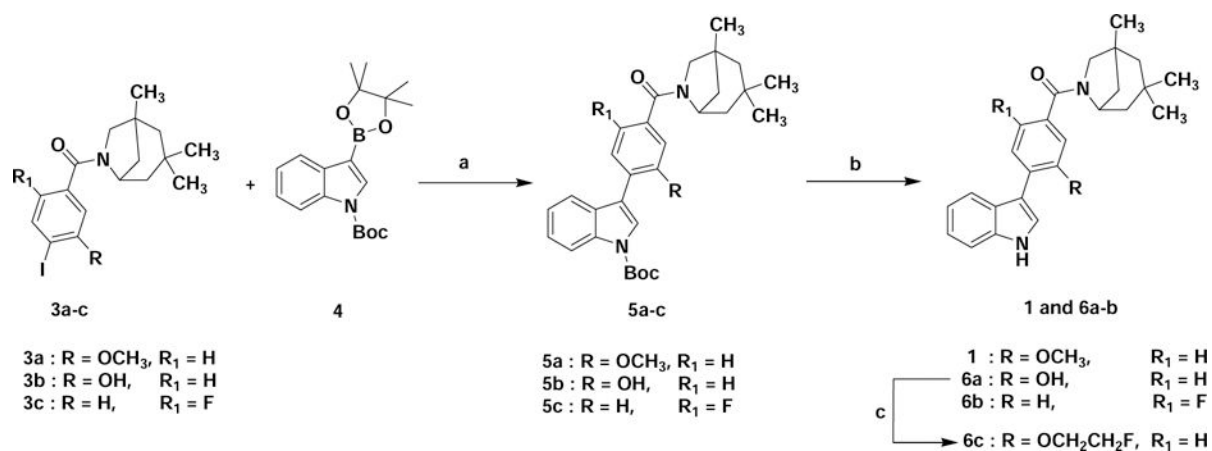


Figure 4. Effect of three anesthetics (Propofol, Ketamine and Saffan) on the brain uptake of [^{11}C] (1*S*,5*R*)-**1** in CD-1 mice at 30 min after the radiotracer injection. The anesthetics were injected ip (80 mg/kg), 30 min prior the radiotracer. Data: mean %ID/g tissue \pm SD (n = 3). Abbreviations: Hipp, hippocampus; Ctx, cortex; SEP, septum; Rest, the rest of brain. All three anesthetics increased the variability of the radiotracer uptake. The radiotracer uptake was significantly lower in the hippocampus in mice treated with Propofol. * $P < 0.01$, significantly different from control (ANOVA).

**Scheme 1.**

Synthesis of key intermediates.

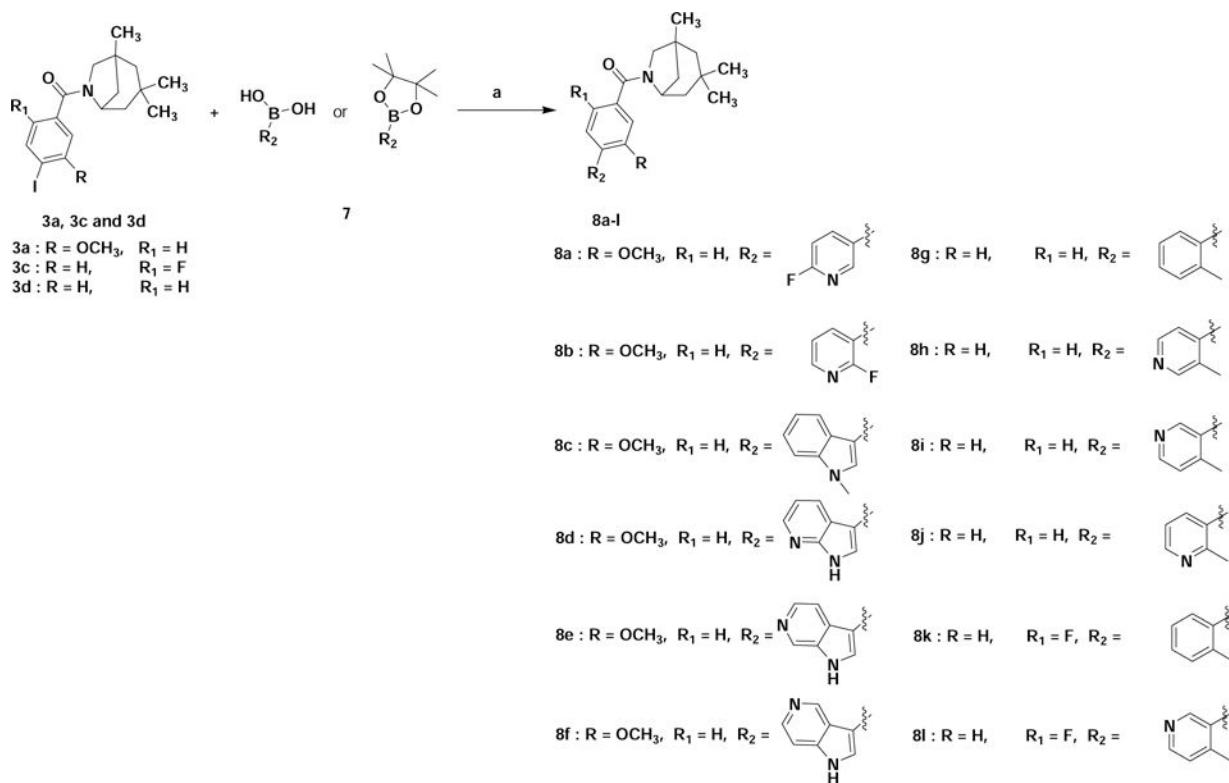
Reagents and conditions: a) EDC, HOBT, DIEA, DMF

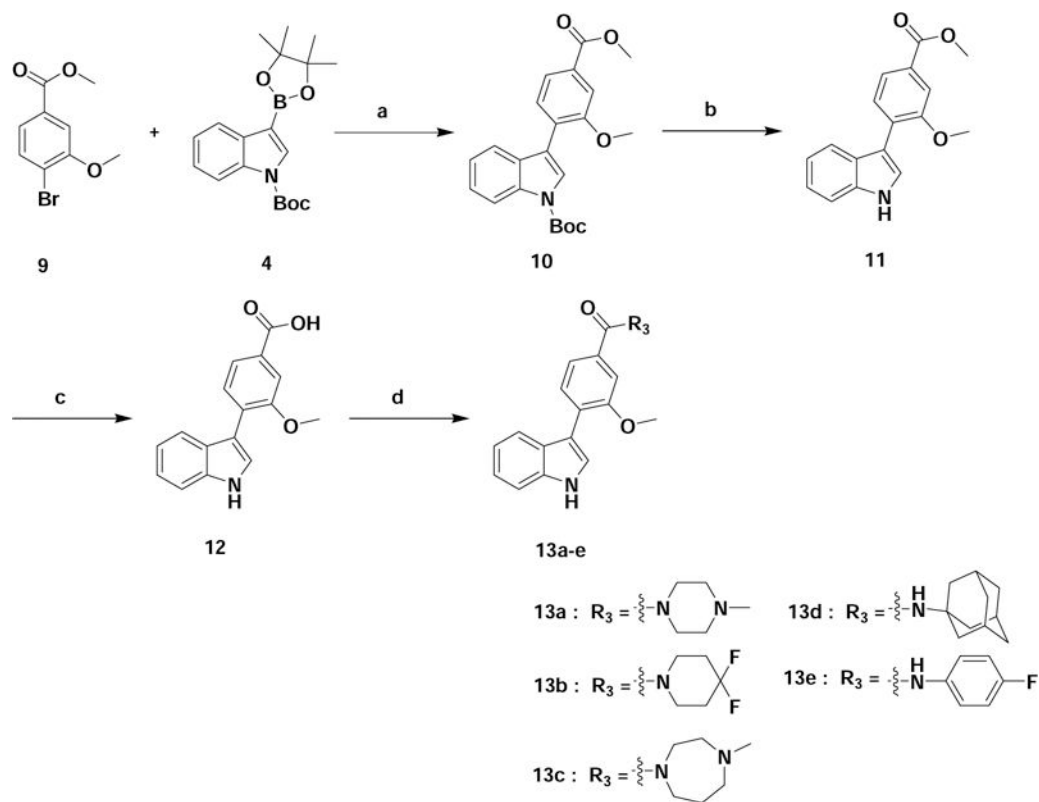
**Scheme 2.**

Synthesis of compounds **1** and **6a-c**.

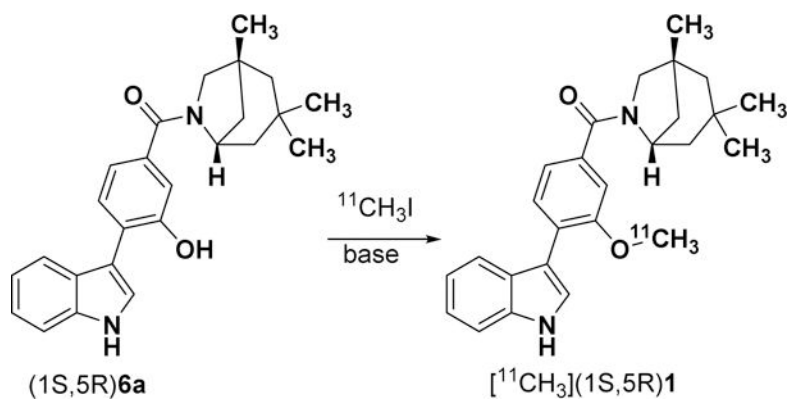
Reagents and conditions: a) Pd(dppf)Cl₂.DCM, Na₂CO₃, 1,4-Dioxane/H₂O; b) TFA, MC;

c) 2fluoroethyl Tosylate, Cs₂CO₃, DMF.

**Scheme 3.**Synthesis of vasopressin ligands **8a-l**.**Reagents and conditions:** a) Pd(dppf)Cl₂.DCM, Na₂CO₃, 1,4-Dioxane/H₂O.

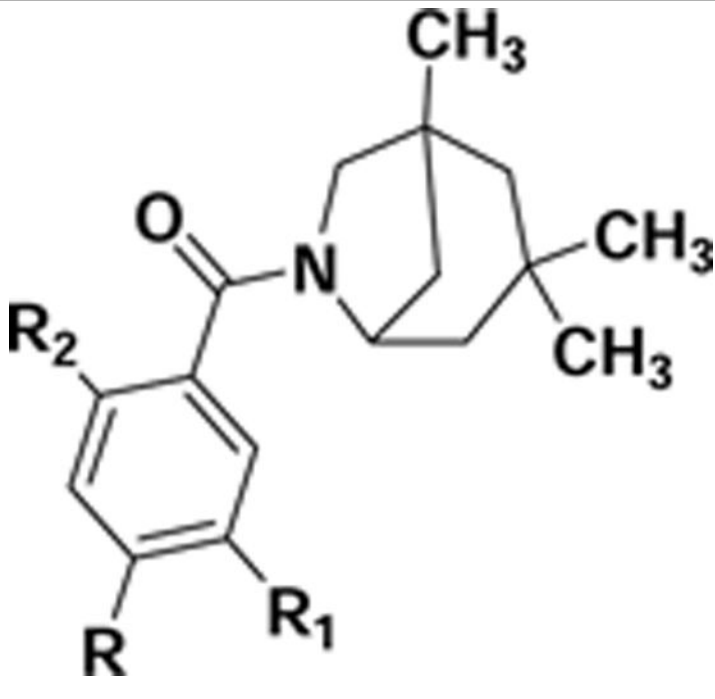
**Scheme 4.**Synthesis of compounds **13a-e**.

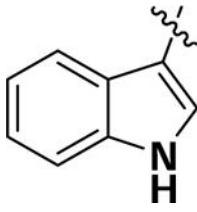
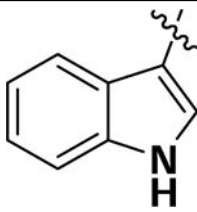
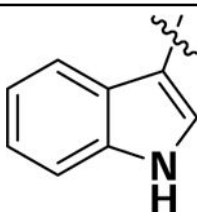
Reagents and conditions: a) Pd(dppf)Cl₂.DCM, Na₂CO₃, 1,4-Dioxane/H₂O; b) TFA, MC; c) LiOH, THF/ H₂O; d) EDC, HOBT, DIEA, DMF.

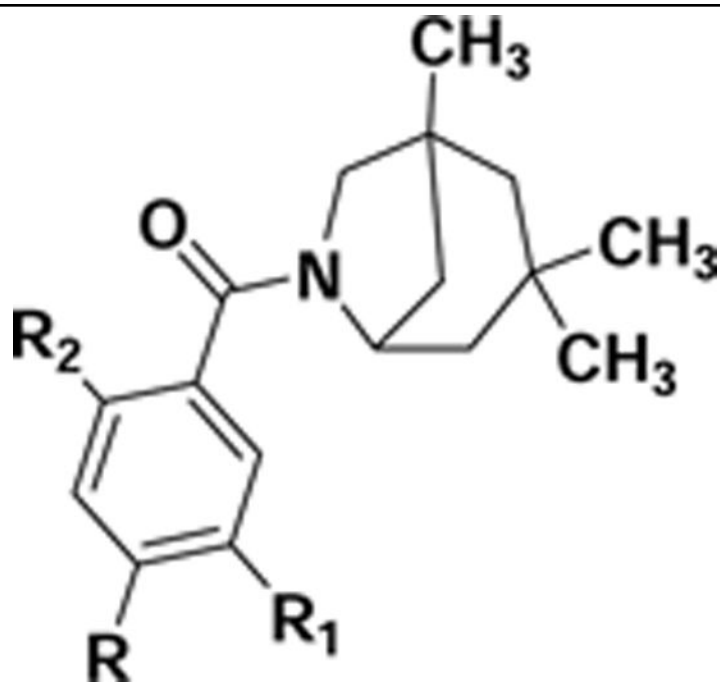


Scheme 5.
Radiosynthesis of [^{11}C](1S,5R)-1

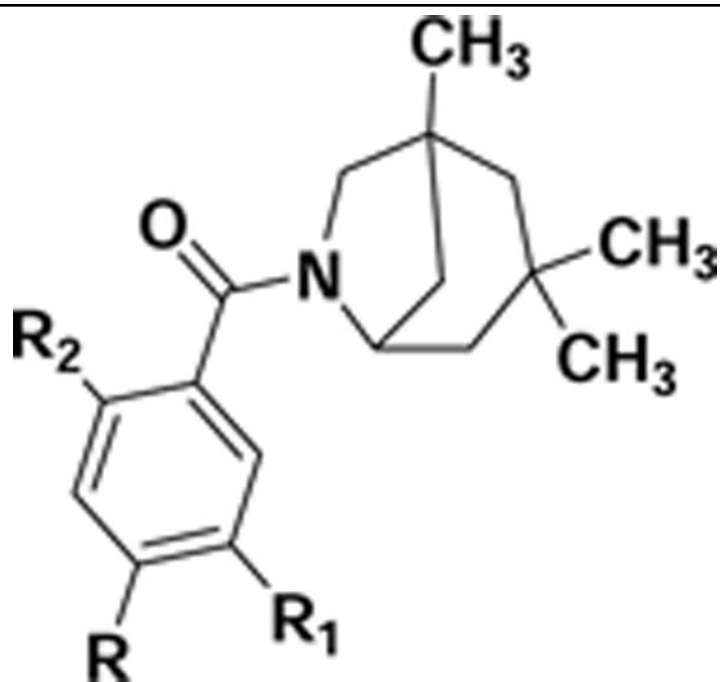
Table 1.

Binding inhibition and lipophilicities of V_{1a} ligands **1**, **6b-c**, **8a-l**.


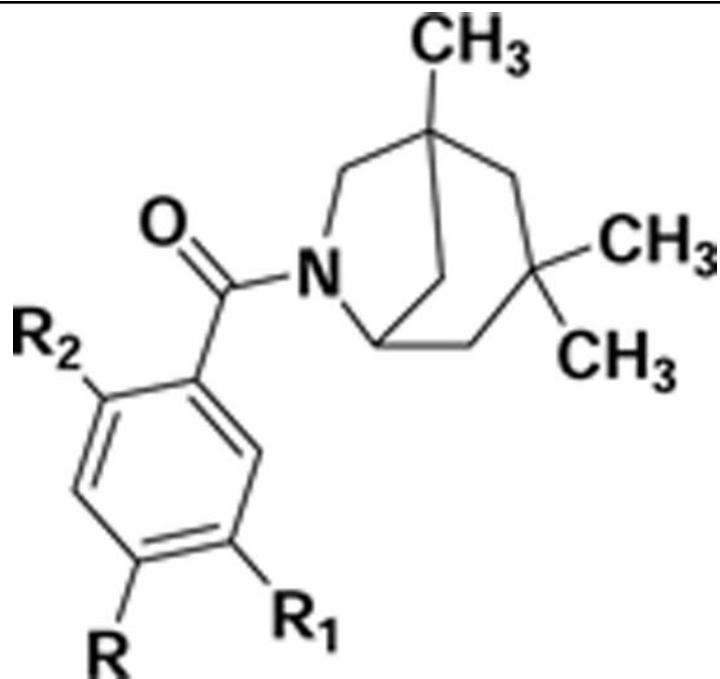
Compounds	R	R ₁	R ₂	logD _{7,4}	% Binding inhibition ^a (concentration)	
					(10 ⁻⁹ M)	(10 ⁻⁸ M)
(1 <i>S</i> ,5 <i>R</i>)- 1		OCH ₃	H	4.7	51.4	87.9 ^b
(1 <i>R</i> ,5 <i>S</i>)- 1		OCH ₃	H	4.7	7.1	8.9 ^b
6b		H	H	4.8	33.4	77.1



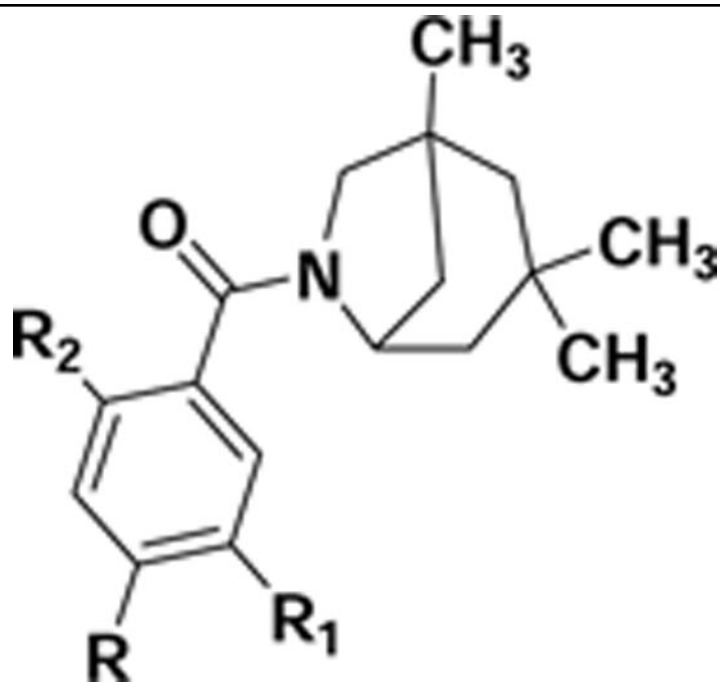
Compounds	R	R ₁	R ₂	logD _{7,4}	% Binding inhibition ^a (concentration)	
					(10 ⁻⁹ M)	(10 ⁻⁸ M)
6c		OCH ₂ CH ₂ F	H	4.9	45.1	92.6
8a		OCH ₃	H	3.9	2.9	33.9
8b		OCH ₃	H	4.0	9.7	16



Compounds	R	R ₁	R ₂	logD _{7,4}	% Binding inhibition ^a (concentration)	
					(10 ⁻⁹ M)	(10 ⁻⁸ M)
8c		OCH ₃	H	6.0	1.8	18.7
8d		OCH ₃	H	2.9	4.4	28.7
8e		OCH ₃	H	3.5	-4.7	44.2



Compounds	R	R ₁	R ₂	logD _{7,4}	% Binding inhibition ^a (concentration)	
					(10 ⁻⁹ M)	(10 ⁻⁸ M)
8f		OCH ₃	H	2.8	5.2	39.5
8g		H	H	5.0	23.7 ^c	84.3
8h		H	H	4.4	10.5	28.9
8i		H	H	4.4	12.8	43.9



Compounds	R	R ₁	R ₂	logD _{7,4}	% Binding inhibition ^a (concentration)	
					(10 ⁻⁹ M)	(10 ⁻⁸ M)
8j		H	H	4.4	-6.6	18.2
8k		H	F	5.8	22.8	81.2
8l		H	F	4.5	2.4	19.8

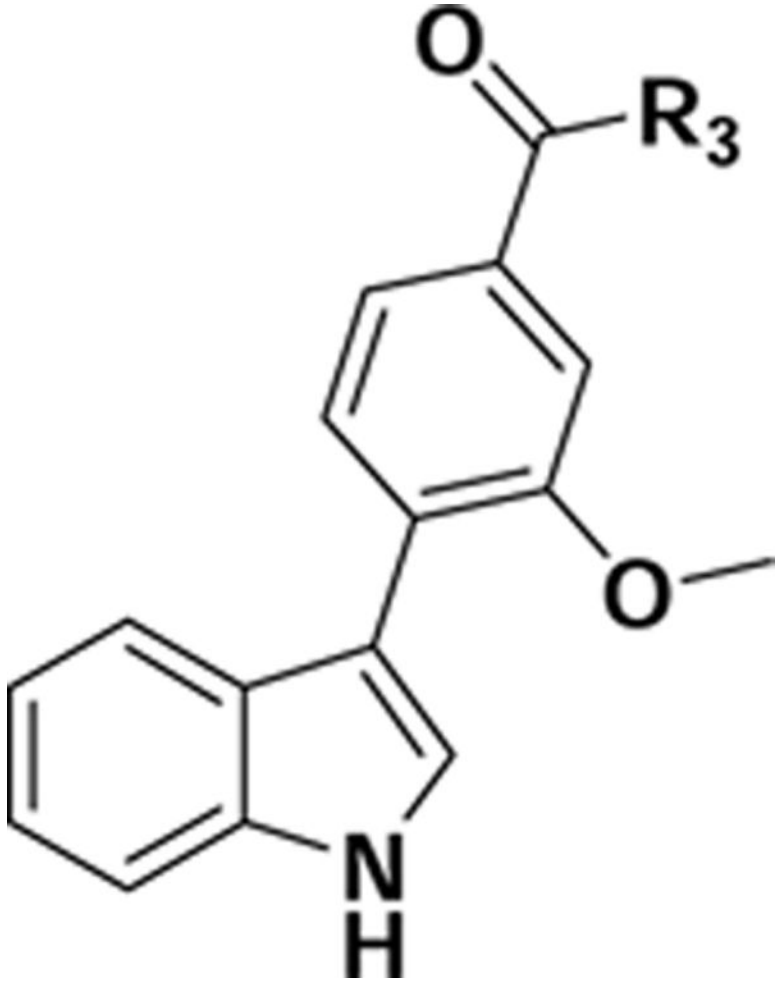
^aValues are the means of two experiments, each in duplicate.

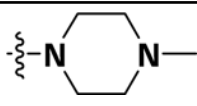
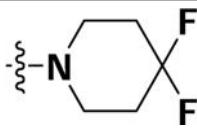
^bThe V_{1a} inhibition binding affinity constant values of (1*S*,5*R*)-**1** (K_i = 0.66 nM) and (1*R*,5*S*)-**1** (K_i > 10 nM) were determined in a separate binding assay. This result is in agreement with previously published data for (1*S*,5*R*)-**1** (K_i = 0.1 nM) [22].

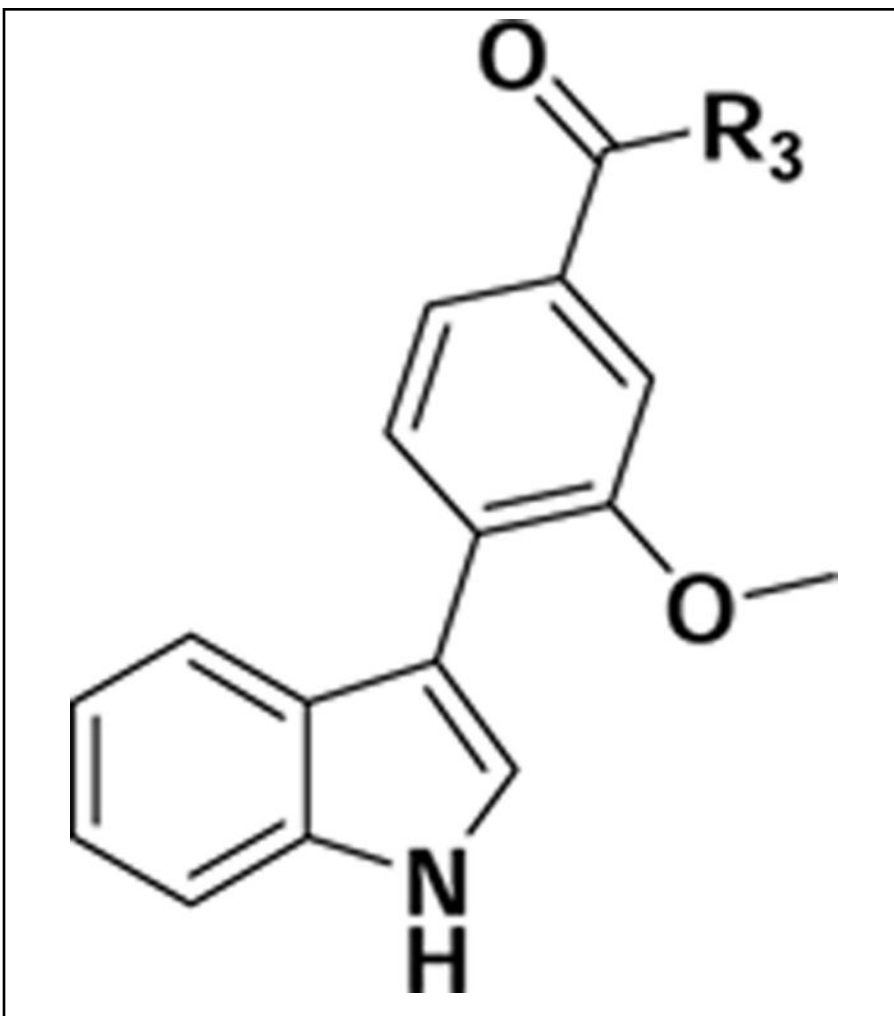
^cCompound **8g** was described previously (K_i = 0.05 nM) [22].

Table 2.

Binding Affinities of the Derivatives 13a-e.



Compounds	R	logD _{7,4}	% Binding inhibition ^a (concentration)	
			(10 ⁻⁹ M)	(10 ⁻⁸ M)
13a		0.7	15.7	4.7
13b		1.6	13.7	9.0



Compounds	R	logD _{7,4}	% Binding inhibition ^a (concentration)	
			(10 ⁻⁹ M)	(10 ⁻⁸ M)
13c		0.2	5.7	6.2
13d		5.8	7.4	4.8
13e		3.2	5.0	4.6

^aValues are the means of % inhibitions of two independent experiments, each in duplicate.

Table 3.Regional distribution of [¹¹CH₃](1*S*,5*R*)-1 in CD1 male mouse brain (mean %ID/g tissue ± SD, n=3)

	5 min	15 min	30 min	60 min
Septum	4.71±0.57	2.70±0.06	1.94±0.76	0.86±0.18
Hippocampus	3.37±0.32	2.17±0.06	1.62±0.52	0.75±0.18
Cortex	4.44±0.52	2.41±0.08	1.52±0.52	0.60±0.08
Rest of brain	3.95±0.35	2.34±0.02	1.54±0.52	0.65±0.12

Author Manuscript

Author Manuscript

Author Manuscript

Author Manuscript